UNIVERSIDADE FEDERAL DE SANTA CATARINA
CAMPUS JOINVILLE
PROGRAMA DE PÓS-GRADUAÇÃO EM ENGENHARIA E CIÊNCIAS MECÂNICAS

Luana Bavaresco Rossari

Numerical Simulation of Tylose Packages Freezing Time

Joinville
2021

Luana Bavaresco Rossari

Numerical Simulation of Tylose Packages Freezing Time

Dissertação submetida ao Programa de Pós-Graduação em Engenharia e Ciências Mecânicas da Universidade Federal de Santa Catarina para a obtenção do título de Mestre em Engenharia e Ciências Mecânicas.
Orientadora: Prof. Talita Sauter Possamai, Dra.
Coorientador: Prof. Kleber Vieira de Paiva, Dr.

Joinville
2021

Ficha de identificação da obra elaborada pelo autor,
através do Programa de Geração Automática da Biblioteca Universitária da UFSC.

Rossari, Luana Bavaresco
Numerical Simulation of Tylose Packages Freezing Time
Joinville / Luana Bavaresco Rossari ; orientadora, Talita Sauter Possamai, coorientador, Kleber Vieira de Paiva, 2021.
85 p.

Dissertação (mestrado) - Universidade Federal de Santa Catarina, Campus Joinville, Programa de Pós-Graduação em Engenharia e Ciências Mecânicas, Joinville, 2021.

Inclui referências.

1. Engenharia e Ciências Mecânicas. 2. Simulação numérica. 3. Tylose. 4. Transferência de calor. 5. Modelagem de sistemas. I. Sauter Possamai, Talita. II. Vieira de Paiva, Kleber. III. Universidade Federal de Santa Catarina. Programa de Pós-Graduação em Engenharia e Ciências Mecânicas. IV. Título.

Luana Bavaresco Rossari

Numerical Simulation of Tylose Packages Freezing Time

O presente trabalho em nível de mestrado foi avaliado e aprovado por banca examinadora composta pelos seguintes membros:

Prof. Diogo Lôndero da Silva, Dr.
Universidade Federal de Santa Catarina

Prof. Fabiano Gilberto Wolf, Dr.
Universidade Federal de Santa Catarina

Prof. Paulo Sérgio Berving Zdanski, Dr.
Universidade do Estado de Santa Catarina

Certificamos que esta é a **versão original e final** do trabalho de conclusão que foi julgado adequado para obtenção do título de Mestre em Engenharia e Ciências Mecânicas.

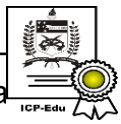

Documento assinado digitalmente
Rafael de Camargo Catapan
Data: 07/02/2021 18:06:20-0300
CPF: 029.036.159-18

Prof. Rafa
Coordenador do Programa

Documento assinado digitalmente
Talita Sauter Possamai
Data: 07/02/2021 14:11:31-0300
CPF: 052.039.319-84

Prof. Talita Sauter Possamai, Dra.
Orientadora

Joinville, 2021.

AGRADECIMENTOS

Aos meus pais, Ivete e Odair, por sempre me incentivarem e apoiarem para que eu pudesse alcançar meus objetivos. À Heloísa, pelo seu apoio como irmã e contribuição como colega de profissão.

À minha orientadora, Prof. Talita Sauter Possamai, pelo conhecimento, apoio e por acreditar na realização deste trabalho.

À Yasmim Niehues Silvano pela parceria nas aulas, trabalhos e dias de estudo durante essa jornada.

Aos meus colegas de trabalho Marcos Heinzle, Vinicius Bianchezzi, Emerson Heck, Luis Dalbem, Mariana Bianchi e Lincoln Garcia que de alguma forma contribuíram para que a realização desse trabalho fosse possível.

Ao Rogério Rodrigues Jr pelo conhecimento compartilhado e pelas incontáveis discussões, sem a sua contribuição este trabalho não seria possível.

RESUMO

A tylose é um material composto majoritariamente por água e metilcelulose usado como modelo de alimento em experimentos devido a similaridade das suas caracaterísticas termofísicas às da carne magra. Este trabalho apresenta o estudo do tempo de congelamento de pacotes de tylose de formato retangular. Testes experimentais foram realizados utilizando um refrigerador doméstico *no-frost* como o meio para congelamento dos pacotes de tylose, os testes consideraram dois pacotes sozinhos e duas pilhas com dois pacotes cada. Uma abordagem combinando um modelo CFD (Dinâmica dos Fluidos Computacional), um modelo 1D e um modelo de otimização foi usado para estimar as propriedades termofísicas do material de tylose. Um modelo simplificado de CFD considerando apenas o compartimento do freezer foi utilizado para simular as condições do teste e definir o coeficiente global de transferência de calor (UA) de cada uma das superfícies dos pacotes presentes nos testes experimentais. Então um modelo 1D representando o pacote como uma combinação de um elemento capacitor térmico, de elementos condutores térmicos e elementos convectivos foi construído para simular o tempo de congelamento. Como as propriedades termofísicas destes pacotes são desconhecidas, um modelo de otimização foi construído para defini-las usando uma função objetivo que buscava reduzir a diferença entre os resultados experimentais obtidos *in loco* e simulados em pontos definidos durante o tempo de congelamento. Os resultados mostraram uma boa correlação para os pacotes sozinhos com as propriedades termofísicas obtidas através da otimização que não considerou os pacotes empilhados, mostrando boa aderência da curva de congelamento e uma diferença de -2.4% e -3.2% entre os testes experimentais e a simulação. Contudo, o resultado dos pacotes empilhados mostrou uma diferença maior, muito provavelmente devido a dificuldade na modelagem do contato entre os pacotes e também entre o pacote e a superfície do compartimento congelador.

Palavras-chave: Tylose, Mudança de Fase, Simulação Numérica, Dinâmica dos Fluidos Computacional, Modelica, Modelagem de Sistemas.

RESUMO EXPANDIDO

Introdução

O congelamento é uma técnica amplamente utilizada na indústria alimentícia para garantir a preservação dos alimentos por um longo período, mantendo ao mesmo tempo a qualidade dos mesmos. Alimentos como a carne são altamente perecíveis e necessitam de um processo e um sistema de congelamento eficiente para uma melhor preservação, um menor consumo de energia do sistema e uma baixo custo. Para projetar um sistema de congelamento eficiente são necessários testes com os diferentes tipos de produtos que serão submetidos ao processo de congelamento, o que pode ser feito de forma experimental ou através de simulação. Simulações podem auxiliar na avaliação de diferentes aspectos do congelamento, como a frente de congelamento, tempo de congelamento e temperatura de congelamento em regime permanente, porém para realizar esses estudos as propriedades termofísicas dos produtos armazenados precisam estar definidas. A determinação dessas propriedades pode ser complexa, pois a composição de produtos agrícolas e marinhos pode variar muito e suas propriedades termofísicas tendem a ser imprecisas. Dessa forma, um material análogo conhecido como Tylose, um gel composto de metilcelulose com propriedades termofísicas similares a da carne magra, é amplamente utilizado para estas avaliações. Previsão do tempo de congelamento através de simulação é um tema amplamente estudado e embora várias abordagens tenham sido desenvolvidas ao longo dos anos, muitos dos estudos apresentam desvantagens como o alto tempo computacional das simulações transientes e a determinação do coeficiente convectivo, dificultando a aplicação em larga escala na indústria.

Objetivos

O objetivo principal deste estudo é desenvolver um método para previsão do tempo de congelamento combinando modelos de CFD e 1D de modo que este seja viável em termos de tempo computacional, com uma possível aplicação na indústria. Os objetivos específicos são: realizar testes experimentais em um refrigerador doméstico para aquisição de dados do tempo de congelamento das amostras dos pacotes de tylose dentro do compartimento congelador; realizar uma simulação CFD em regime permanente para definir o coeficiente global de transfrência de calor (UA) para as superfícies dos pacotes; usar os valores de UA e as propriedades termofísicas como condições de contorno no modelo 1D para simular o tempo de congelamento dos pacotes; realizar um estudo de otimização para caracterizar as propriedades termofísicas da tylose.

Metodologia

Testes experimentais foram realizados em um refrigerador *top mount no frost*, que tem por princípio de funcionamento o fluxo de ar forçado, com os pacotes de tylose ar-

mazenados no compartimento congelador considerando uma configuração específica. O objetivo dos testes foi obter dados da condição de funcionamento do refrigerador para serem aplicados como condições de contorno no modelo numérico e também obter resultados do tempo e da curva de congelamento dos pacotes para correlação. As temperaturas medidas no teste foram: temperatura do centro dos pacotes, temperatura ambiente da câmara de testes, temperatura do fluxo de ar, temperatura do tubo do evaporator e a temperatura no centro geométrico do compartimento congelador acima e abaixo da prateleira. A temperatura do fluxo de ar foi utilizada como condição de contorno na simulação 1D e a temperatura do evaporator na simulação CFD. O domínio do modelo de simulação considerou apenas a parte do compartimento congelador devido a grande quantidade de elementos da malha, uma vez que o modelo considera o evaporator tubo-aletado. As simulações foram realizadas no software comercial ANSYS Fluent. Foram aplicadas as seguintes condições de contorno na simulação: temperatura e coeficiente convectivo prescritos nas paredes externas do refrigerator; condição adiabática nas superfícies que fazem contato com o refrigerador e foram removidas; valor de vazão mássica na superfície em contato com os dutos de retorno para especificar a quantidade de ar que retornaria do compartimento refrigerador; no duto de insuflamento para o refrigerador foi considerada uma pressão manométrica igual a zero; no interior dos tubos foi aplicada uma temperatura e o coeficiente convectivo prescritos;para representar o movimento de rotação do ventilador foi utilizado o modelo MRF. Um estudo de refino de malha foi feito avaliando-se o tamanho da malha superficial em contato com os pacotes e também o tamanho da malha volumétrica do ar do freezer. Foram realizados quatro testes para definir o melhor custo benefício em termos de quantidade de elementos e também em termos do resultado da quatidade de troca de calor nas superfícies dos pacotes.

Um modelo 1D de transferência de calor representando o pacote de tylose foi construído utilizando o software OpenModelica, com equações modificadas para modelar a mudança de fase, com objetivo de estimar o tempo de congelamento . O modelo é composto pelos seguintes componentes: um capacitor de calor, condutores térmicos e convectivos para cada uma das superfícies do pacote. Para os pacotes empilhados foi construído um modelo similar considerando o contato entre os pacotes. Os dados de entrada necessários para simular o processo de congelamento são: temperatura do ar do compartimento estimada nos testes experimentais, os valores de UA e as propriedades termofísicas da tylose. Como as propriedades termofísicas dos pacotes de tylose utilizados nos testes experimentais não eram conhecidas, uma otimização usando o software modeFRONTIER foi realizada para estimá-las. A função objetivo definida para a otimização foi definir os valores das variáveis que resultassem na menor diferença entre os pontos nas curvas experimentais e simuladas para os mesmos pontos no tempo. Para que posteriomente houvessem valores experimentais para

a validação foram considerados somente os pacotes das posições 01, 05 e 06 na otimização.

Resultados e Discussão

Os resultados do estudo de refino de malha apresentaram uma baixa variação e definiu-se o tamanho da malha superficial de 4 mm e da malha volumétrica de 6 mm como o melhor custo-benefício para o caso. Os valores de UA para este caso foram calculados e mostraram-se condizentes com o comportamento físico esperado devido a posição de cada pacote. Além disso compararam-se os valores experimentais e simulados para a temperatura do ar medida no centro geométrico acima e abaixo da prateleira do compartimento congelador, os quais mostraram uma boa correlação.

Os valores de UA encontrados foram aplicados como valores de entrada no modelo 1D e uma otimização foi realizada para encontrar as propriedades termofísicas dos pacotes de tylose. A primeira otimização foi realizada considerando o modelo 1D no qual não havia resistência de contato entre os pacotes empilhados. O resultado apresentou um comportamento inesperado para o pacote no topo da pilha, um degrau foi observado na parte de solidificação da curva do pacote na posição 05 aproximadamente no mesmo ponto no tempo em que o pacote na posição 06 finalizava a parte de mudança de fase. Isso ocorreu devido ao artifício de modelagem aplicado no componente de condução térmica que realiza uma média da temperatura da superfície e do centro do pacote, porém no caso dos pacotes empilhados este realizou uma média entre a superfície do pacote inferior e superior. Para mitigar esse efeito no contato entre os dois pacotes empilhados uma resitência térmica foi incluída entre esses pacotes.

A otimização das propriedades termofísicas foi novamente realizada considerando duas abordagens: a primeira onde a função objetivo buscou minimizar a diferença entre testes experimentais e simulação para os pacotes em três posições simultaneamente (posições 01, 05 e 06) e a segunda onde se buscou otimizar apenas o pacote sozinho (posição 01). Para a primeira abordagem observou-se que a fase líquida apresentou boa correlação entre as curvas experimentais e simuladas, porém a parte de mudança de fase e solidificação não apresentaram boa correlação em relação a curva e o tempo de tais fases. Na segunda abordagem também foi observada uma boa correlação das curvas na fase líquida para os pacotes em todas as posições. Avaliando os pacotes sozinhos nas posições 01 e 02, observou-se uma boa aderência das curvas para a parte de mudança de fase e de solidificação e também a concordância dos resultados do tempo total para o congelamento. Por outro lado, os resultados do pacotes empilhados não apresentaram boa correlação. Para os pacotes nas posições 04 e 06, o comportamento da curva apresenta similaridade entre as curvas experimentais e as simuladas para a fase de congelamento, porém não o tempo total de congelamento não foi corretamente previsto. Essa diferença pode ter ocorrido devido

a interação entre os pacotes e a interaçõa entre a superfície do congelador em contato com os pacotes que não foi capturada no modelo. Os pacotes nas posições 03 e 05 não apresentaram similaridade entre as curvas na parte de mudança de fase e sólida. Avaliando as curvas experimentais para os pacotes nessas posições é possível observar que o comportamento da curva após o período de mudança de fase é diferente dos pacotes nas outras posições, apresentando uma transição suave ao contrário do que observa-se nos pacotes nas outras posições. Esse comportamento pode ter ocorrido devido a influência do pacote inferior da pilha e o modelo não é capaz de capturar esse efeito. Avaliou-se também o tempo total para o congelamento considerando uma temperatura inicial de 20°C e final de -18°C. A simulação considerando as propriedades obtidas através da segunda abordagem de otimização mostrou bons resultados para os pacotes sozinhos nas posições 01 e 02 com variação de -2.4% e -3.2% respectivamente entre dados experimentais e simulação, porém uma diferença maior foi observada para os pacotes empilhados reforçando a necessidade de melhoria na modelagem. Os resultados da simulação considerando as propriedades obtidas com a primeira abordagem de otimização não se mostram tão distantes dos valores experimentais, variando entre -1.5% e 11.9%, porém como visto anteriormente as curvas não representam corretamente o comportamento dos pacotes. Dessa forma considerando o tempo de congelamento e também o comportamento das curvas pode-se afirmar que as propriedades termofísicas que apresentaram os melhores resultados foram as obtidas através da segunda abordagem de otimização, sendo estas: Tsl = -1°C, DTs = 0.57°C, Hsl = 123859.9 J/Kg, Cpl = 3059.87 J/KgK, Cps = 3187.56 J/KgK, kl = 0.5232 W/mK e ks = 0.7383W/mK.

Conclusão

O presente estudo propôs um método numérico combinando a aplicação de um modelo CFD, um modelo 1D e um modelo de otimização para prever o tempo de congelamento de pacotes de tylose. Testes experimentais foram realizados com pacotes de tylose submetidos ao congelamento em dois refrigeratores *top mount no frost* para obtenção de dados para a correlação do modelo numérico a ser desenvolvido. O experimento considerou pacotes sozinhos e também empilhados dentro do compartimento congelador. Um modelo CFD foi utilizado para definir a transferência de calor em cada uma das superfícies dos pacotes através da simulação do fluxo de ar no compartimento congelador do produto. Utilizando os resultados de transferência de calor, as temperaturas de insuflamento do compartimento e a temperatura prescrita nos pacotes calculou-se os valores de UA para as superfícies dos pacotes. O modelo 1D utilizou esses valores de UA como dados de entrada para as equações de convecção. A transferência de calor por condução e a capacitância térmica também foram modeladas e customizadas para representarem a curva de mudança de fase. Utilizando os resultados dos modelos de

CFD e 1D uma otimização foi realizada para definir as propriedades termofísicas que melhor representam os pacotes de tylose. A primeira otimização mostrou resultados inesperados na curva do pacote superior da pilha, este sofreu influência da temperatura do pacote inferior da pilha, portanto um resistência de contato foi adicionada entre os pacotes empilhados. A segunda otimização utilizou duas abordagens: uma buscando minimizar a função objetivo considerando três pacotes (um sozinho e dois empilhados) e a outra minimizar a função objetivo apenas para o pacote sozinho. Considerando as propriedades obtidas com a primeira abordagem, os resultados de simulação não apresentaram uma boa correlação com os dados experientais, em especial na parte de mudança de fase e solidificação. Os resultados da simulação realizada com as propriedades obtidas através da segunda abordagem apresentam uma boa correlação da curva e do tempo de congelamento para os pacotes sozinhos, porém os resultados para os pacotes empilhados não apresentaram boa correlação. O método proposto se mostrou capaz de prever a curva e o tempo de congelamento para pacotes não empilhados com um baixo esforço e tempo computacional comparado à uma simulação CFD transiente. Para os pacotes empilhados, o modelo 1D necessita ser aperfeiçoado de forma a capturar efeitos importantes que ocorrem devido ao arranjo físico.

Palavras-chave: Tylose, Mudança de Fase, Simulação Numérica, Dinâmica dos Fluidos Computacional, Modelica, Modelagem de Sistemas.

ABSTRACT

Tylose is a material composed mostly of water and methyl cellulose used as food model in experiments due to its thermophysical properties similarity to the lean beef. This work presents a study of the freezing time of tylose rectangular shaped packages. Experimental tests were performed using a no-frost household refrigerator as the mean for freezing the tylose packages, the test considered two standalone packages and two stacks of two packages each. An approach combining a CFD (Computer Fluid Dynamics) model, a 1D model and an optimization model were used to estimate the thermophysical properties of the tylose material. A simplified CFD model considering only the freezer compartment was used to simulate the tested conditions and define the global heat transfer coefficient (UA) for each of the surfaces of the packages present in the experimental tests. Then a 1D model representing the package as a combination of a thermal capacitor element, thermal conductor elements and convective elements was built to simulate the freezing time. Since the thermophysical properties for these packages are unknown an optimization model was built to define them using a objective function that aimed to reduce the difference between the experimental and simulated results at defined points along the freezing time. The results showed a good correlation for the standalone packages with the thermophysical properties obtained from the optimization that did not consider the stacked packages, showing a good adherence of the freezing curve and a difference of -2.4% and -3.2% between experimental and simulation tests. However the stacked packages results showed a larger difference most probably due to a gap in the modeling of the contact between packages and also between package and freezer compartment surface.

Keywords: Tylose, Phase Change, Numerical Simulation, Computational Fluid Dynamics, Modelica, System Modeling.

LIST OF FIGURES

LIST OF TABLES

LIST OF ABBREVIATIONS AND ACRONYMS

CAD	Computer Aided Design
CFD	Computational Fluid Dynamics
DNS	Direct Numerical Simulation
IEC	International Electrotechnical Commission
ISO	International Organization for Standardization
LES	Large Eddy Simulation
MSE	Measurement System Evaluation
ODE	Ordinary differential equation
RANS	Reyonolds Average Navier-Stokes
SPC	Stable, Predictible and Consistent
UCL	Upper Control Limit

LIST OF SYMBOLS

A	Package surface area [m²]
A_r	Package contact area [m²]
N	Number of measurement units [-]
B	Body forces [N/m³]
Cp	Specific heat [J/KgK]
Cpl	Specific heat at liquid state [J/KgK]
Cps	Specific heat at solid state [J/KgK]
DTs	Phase change temperature range [°C]
fs	Liquid mass fraction [-]
h_0	Total enthalpy [J/Kg]
Hsl	Phase change enthalpy [J/Kg]
k	Thermal conductivity [W/mK]
kl	Thermal conductivity at liquid state[W/mK]
ks	Thermal conductivity at solid state[W/mK]
k_r	Thermal conductivity of the plastic [W/mK]
L	Distance from the center to the surface of the package [m]
L_r	Thickness of the plastic wrapping [m]
m	Mass [-]
n	Number of points used in the optimization [-]
Nu	Nusselt number [-]
p	Pressure [Pa]
Q	Total heat transfer [W]
R	Range [-]
R_g	Specific constant of gas [J/KgK]
Sh	Sherwood number [-]

t	Time [s]
T	Temperature [K]
Ta	Temperature at port a [K]
Tb	Temperature at port b [K]
Tsl	Phase change temperature [°C]
S_h	Source term [W/m³]
u	Velocity in x coordinate [m/s]
UA	Global heat transfer coefficient [W/m²K]
v	Velocity in y coordinate [m/s]
x	Coordinate direction [m]
$\bar{X}$	Sample mean [-]
u	Velocity in z coordinate [m/s]

Greek Letters

Δ	Difference between points [-]
ρ	Density [Kg/m³]
τ	Stress tensor [N/m²]
δ_{ij}	Kronecker delta [-]
μ	Dynamic viscosity [Ns/m²]
Γ	Averaging interval [-]
ϕ	Generic instantaneous variable [-]
ϕ'	Generic variable Reynolds fluctuation [-]
σ	Standard deviation [-]

Subscripts

i	Refers to the coordinate axis [x, y, z]
c	Package center

a	Air
surf	Package surface
l	Liquid
s	Solid
sim	Simulation
exp	Experimental
Sum	Sum of values
Pos01	Position 01
Pos02	Position 02
Pos03	Position 03

CONTENTS

1 INTRODUCTION

1.1 MOTIVATION

Freezing is a widely used preservation technique in the food industry once it ensures a long preservation with relatively low impact on product quality (MULOT et al., 2019). In the meat industry, for example, this process is largely used to keep the nutritional value and sensory characteristics of meat (CASTRO-GIRÁLDEZ et al., 2014). Since meat is a highly perishable food, the freezing system and process need to be efficient to result in better preservation, lower energy consumption and even cost reduction. In order to design an efficient freezing system, tests need to be performed with different types of products that will be submitted to the freezing process. These tests can be experimental or through simulation.

Simulation tests can be performed to evaluate different aspects of the freezing process, such as freezing front, freezing temperature at a steady state condition and freezing time. These evaluations help to improve the systems airflow distribution and temperature, and also to verify if devices like refrigerators and freezers are following regulating standards.

To perform these simulations the thermophysical properties of the stored products, like phase change enthalpy, density and thermal conductivity, must be available to be used as inputs in the models. However, this may be difficult because the composition of agricultural and marine products can vary between species and varieties, which would make the work of determining the thermophysical properties hard and inefficient (SIMPSON; CORTÉS, 2003). Therefore, since food materials tend to have a wide variation in the composition, their thermal property data is usually imprecise, so analogues are commonly used in freezing and thawing experiments (CLELAND, 1985). The most widely analogue used is a food model known as tylose, a methyl cellulose gel with thermophysical properties similar to lean beef.

Prediction of freezing time is widely studied, and several simulation approaches have been developed along the years. Recently, (ZILIO et al., 2018) used a simplified approach applying a melting-solidification routine from STAR-CCM+ software with user defined functions, for evaluation of local thermophysical properties, and a single average value for the airside heat transfer coefficient. The approach was used to predict the freezing time at the center of cylindrical samples of chicken breast and provided good results. However, transient 3D turbulent flow simulations are very time consuming compared to steady state simulations and can be prohibitive in industry to evaluate many different designs.

A different approach was proposed by (PHAM; TRUJILLO; MCPHAIL, 2009). The 3D steady state simulations were performed with different velocities and flow directions at a beef carcass in order to have regression equations that were used as boundary

condition in the numerical solution for heat and mass transfer. Then a 2D finite element model was used to solve heat transfer at different cross sections of the carcass and these points were compared with experimental results. For the tests executed in a wind tunnel the agreement with simulation was good, however for the tests conducted in a industrial chiller only qualitative agreements were found since the experimental data had a lot of uncertainty.

Different simulation approaches were proposed along the years, however most of the studies have downsides, such as the computational time in transient simulation, which can be very time consuming restricting the usage in industry approaches and the heat transfer coefficient determination for more complex geometries which are the usual industry cases. So, in order to be able to largely apply simulation to predict freezing time in an industry scale a simpler and more efficient approach needs to be developed.

1.2 OBJECTIVE

The objective of the present study is to develop a freezing time prediction method combining s 3D turbulent flow model, referenced on forwards as CFD model, and a transient heat transfer with phase change model, referenced on forwards as 1D model, applied to tylose packages. The study aims to deliver a viable computational method in terms of simulation time and with possible industry application.

The specific objectives are:

• Perform experimental tests in a household refrigerator to gather data of the freezing time of tylose packages samples inside the freezer compartment.

• Run a steady state CFD simulation to define the global heat transfer coefficients (UA) for the packages surfaces.

• Use the UA values and the thermophysical properties as boundary conditions in the 1D model to simulate the packages freezing time.

• Perform an optimization study to characterize the thermophysical properties of the tylose package material.

1.3 DISSERTATION STRUCTURE

This dissertation is composed of 8 chapters. Chapter 1 provides a brief introduction of the study discussing the motivation and objective. Chapter 2 presents the tylose material in terms of composition and common usage in the home appliance industry. Chapter 3 presents a literature review with the published work of freezing time prediction methods. Chapter 4 describes the experimental set up, results and a statistical analysis of the data. Chapter 5 describes the governing equations of the system and the turbulence modeling approach. In Chapter 6 the numerical models for CFD, 1D and

optimization are presented. The simulations results are discussed in Chapter 7 and the conclusion of the work with final considerations is presented in Chapter 8.

2 TYLOSE PACKAGES

Tylose is a material composed mostly of water and methyl cellulose. This material is used as food model in experiments since it has thermophysical properties that are similar to lean beef and it also has the ability to be modeled in different shapes (ICIER; ILICALI, 2005), (LLAVE et al., 2016). Due to the tylose thermophysical properties, they are used to model the freezing and thawing processes. This allows tests of these processes to be performed using a more controlled material (OTERO et al., 2006). Average values of the thermo-physical properties found in the literature for the tylose are shown in table 1. Despite being available in the literature, these properties were not applied in the study because there was no information regarding the composition of the tylose material for these references.

Table 1 – Literature average thermophysical properties. Source: (CLELAND; EARLE, 1984), (SUCCAR; HAYAKAWA, 1984)

Property	Description	Succar and Hayakawa (1984)	Cleland and Earle (1984)	Unit
Tsl	Phase change temperature	-0.598		°C
Hsl	Phase change enthalpy		149900	J/Kg
Cpl	Specific heat of liquid	3657	3710	J/Kg°C
Cps	Specific heat of solid state		2010	J/Kg°C
kl	Thermal conductivity at liquid state	0.490	0.61	W/Kg°C
ks	Thermal conductivity at solid state	1.578	1.66	W/Kg°C

Standards for refrigeration appliances require the use of tylose packages for approval tests. ISO 15502 and IEC 62552:2007 standard specify the use of tylose standard packages to perform the following tests:

- Energy consumption test;
- Storage test;
- Freezing test;
- Temperature rise test.

Therefore it is important to have the correct thermal properties for the test packages so they can be modeled through simulation correctly delivering accurate results.

The tylose packages must present the following chemical formulation according to standards ISO 15502 and IEC 62552:2007 for a 1kg package:

- 230 g of oxyethylmethylcellulose
- 764,2 g of water
- 5 g of sodium chloride
- 0,8 g of 6-chloro-m-cresol

For this study the test packages have rectangular parallelepiped shape and they can have different sizes and mass, as shown in table 2. The different dimensions and mass are used to load the compartment in its most critical condition, as loaded as possible.

Table 2 – Tylose test packages dimensions and mass. Source: Author (2020)

Mass (g)	Dimension [height x width x depth] (mm)
125	25 x 50 x 100
250	50 x 50 x 100
500	50 x 100 x 100
500	25 x 100 x 100
1000	50 x 100 x 200

The package with 500g and 50 x 100 x 100 mm is called M-package. This is the only package type which is equipped with a measurement device. It can be either a thermocouple or another temperature measuring device. The remaining package types are not measured during tests and are used only to compose the compartment loads, however every time a 1000g package is used to compose the loading it can be replaced by two M-packages.

3 LITERATURE REVIEW

Food freezing is an important process not only for the food industry, as part of the processing chain, but also for the final consumer, who will need to correctly store the food items in a household refrigerator. Therefore, food freezing time prediction is an important information when designing a refrigerator in order to provide the best airflow and temperature inside the compartment. During the design development of a refrigerator appliance it is not common to use real food in the tests because food does not have a standard composition and shape. Instead, tylose packages are used to provide a standardized comparison internally, during the developments at each manufacturer company, and also externally, to approve the refrigerator of different manufacturers. Therefore, having an efficient refrigerator design will result in a correct food preservation and safety, and also have an equipment that is cost and energy efficient.

Different methods can be applied to predict the freezing time of a given geometry such as analytical, empirical or numerical. A general analytical solution is not available, along the years several analytical models were developed, however the simplifying assumptions in the formulations result in not so accurate models (HOSSAIM; CLELAND; CLELAND, 1992).

An analytical method was presented by (PHAM, 1985), in the work he proposed an approach where a mean conducting path is used in the calculation of Biot's number, which was then applied in a modified Planck's equation for the time to freeze. The method was applied to data presented by previous studies for tylose and lean beef. This method provides a visualization of the shape effect, for example, a cube takes more time to freeze than a sphere with diameter equal to the distance from center to surface. (SALVADORI; MASCHERONI, 1991) developed a simplified analytical model for the prediction of freezing and thawing times. The model was validated for regular geometries, different high water-content food and operating conditions, and the presented accuracy was similar to more complex analytical and numerical methods.

An analysis of several empirical models was performed by (BECKER; FRICKE, 1999), the performance of the models was evaluated by comparing the calculated freezing time with empirical data available in the literature for beef, minced lean beef, tylose gel, among others. Analysis for infinite slabs, infinite cylinders and spheres was done, and based on the average absolute prediction error neither of the models perfomed as the best or worst considering all the geometries.

Numerical methods usage has grown lately, especially because they allow calculation of heat transfer coefficients and/or freezing time for more complex geometries that would be difficult to predict by an analytical or empiral model. The work presented by (ZILIO et al., 2018) used CFD simulations to evaluate the freezing time of chicken breasts. The proposed method consisted of using a commercial software solidifica-

tion/melting routine with thermophysical properties defined through user defined functions, and since phase change simulations are heavy to perform, the simulation was simplified by using average air side heat transfer coefficient values based on experiments. The method was assessed against literature data for tylose infinite slabs and beef meet short cylinder presenting good correlation, then later it was applied for the reference poultry samples also with good correlation.

CFD simulations were also used by (TRUJILLO; PHAM, 2006) in their prediction method. A beef side freezing was simulated using a three-step method in order to reduce the simulation time. The three-step method was proposed by (HU; SUN, 2001) and consists in running a steady state flow field simulation, then calculating the local heat transfer and mass transfer around the geometry surface with the flow information from the steady state simulation, and finally simulating the heat and mass transfer at the beef carcass. The application of this method produced good correlation results. Later, (PHAM; TRUJILLO; MCPHAIL, 2009) simulated this same geometry but considering a new approach, where the beef side was modeled and submitted to several simulation runs that combined different velocities, airflow directions and turbulence intensities to calculate heat side coefficients over different sections of the beef. The results generated regression equations for Nu and Sh expressed in dimensionless numbers. A 2D finite element model was used to solve the heat transport within the product, assuming that there was no heat transfer between sections, and the boundary conditions were calculated with the regressed equations.

From the work presented in this section it is noted that several different methods can result in good correlation between experimental and predicted freezing time for all types of materials. However, there are points that appear as limitations, such as the difficulty to predict the heat transfer coefficient of more complex geometries instead of using only one average value for all the geometry, and another point is related to transient numerical simulations, which can be very time consuming and therefore not being largely applied in the industry. The present work proposes a numerical method aiming a less time consuming approach together with a simpler way for heat transfer coefficient determination for application in refrigeration industry for complex configurations.

4 EXPERIMENTAL TESTS

In order to have correlation data to validate the simulation approach experimental tests were performed. The tests were executed in top mount no-frost refrigerators (figure 1), which by its working principle provide a forced convection airflow. Inside the freezer compartment, tylose packages were placed and therefore submitted to forced convection heat exchange. The objective of the tests was to capture data of the working condition of the refrigerator to be defined as inputs to the numerical model and also to have results regarding the freezing curve and time of tylose packages placed at different positions inside the compartment. The tests were performed in two refrigerator samples considering the same loading configuration.

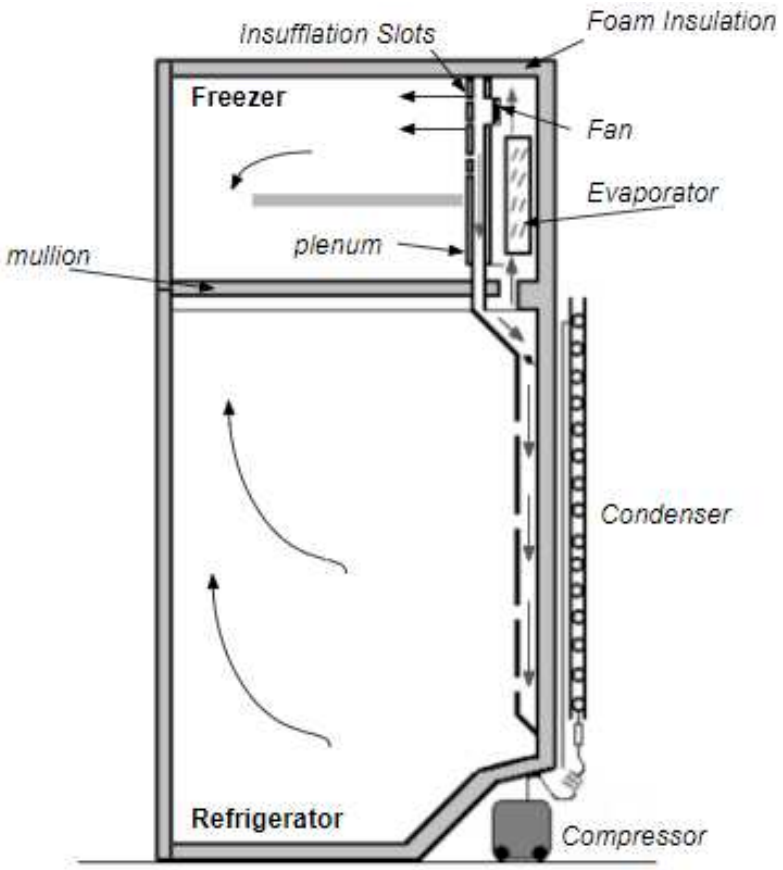

Figure 1 – Top mount no-frost refrigerator. Source: Author (2020)

4.1 MEASUREMENT POINTS

In each refrigerator it was measured the temperature in eleven points listed in table 3 in order to capture information during the freezing process.

Table 3 – Measurement points. Source: Author (2020)

Point	Position
1	Package 01
2	Package 02
3	Package 03
4	Package 04
5	Package 05
6	Package 06
7	Ambient
8	Airflow at insufflation slot
9	Evaporator Tube
10	Geometric center above freezer shelf
11	Geometric center under freezer shelf

Points 1 to 6 are temperature measured in the geometric center of each package and will be used to compare simulation and tests results. Points 8 and 9 will be inputs for the CFD and 1D simulations, presented later on. Points 10 and 11 are comparison points for the CFD simulation. The positions of points 8 to 11 can be obvserved in figure 1. The ambient temperature is measured with two thermocouples located at the vertical and horizontal centerline of the sides of the refrigerator at a distance of 350 mm from the refrigerating appliance (figures 2 and 3) to ensure the stability of the ambient temperature that usually is normative. The airflow temperature is measured at a insufflation slot and the evaporator tube temperature is measured with a thermocouple attached to the tube.

For all temperature measurements were used T type calibrated thermocouples from Omega, with uncertainty of 0.3°C.

4.2 EXPERIMENTAL SET UP

The experiment was executed as a MSE (Measurement System Evaluation) to evaluate if measurement system was able to perform the measurements needed and to verify if packages were similar among each other. The experiment was performed using 500g tylose packages, the M-packages. Six different packages from the same supplier were placed inside the freezer compartment, three in each refrigerator sample. Inside the freezer compartment were also placed three dummy tylose packages (indicated by the white not numbered packages in the figures 4 and 5, not represented in scale) that switched position with the testing ones in order to always have a similar airflow distribution, composing the positions from the set up 1 and 2 (figures 4 and 5). For all the tests, the refrigerator is already on working with empty freezer compartment in steady state condition and then packages were quickly placed inside the compartment for the test start. Each set up was replicated three times. The tests shown in this study were performed at ambient temperature of 43°C controlled by the system operating the

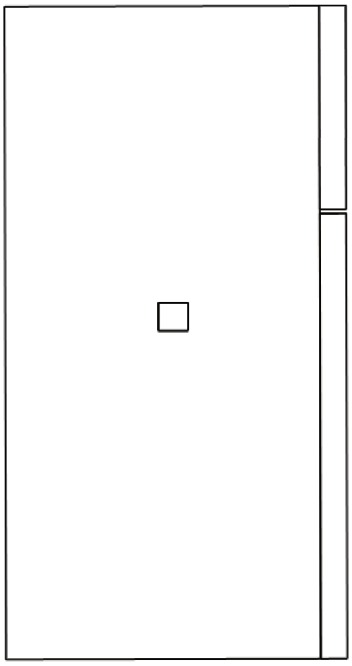

Figure 2 – Ambient temperature thermocouples position - Left side view. Source: Author (2020)

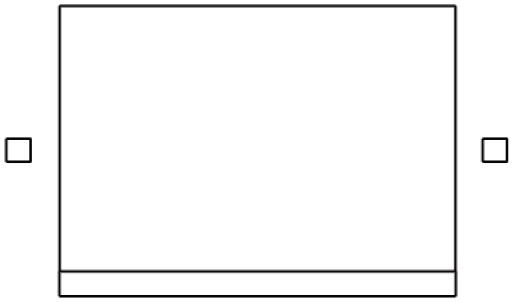

Figure 3 – Ambient temperature thermocouples position - Top view. Source: Author (2020)

testing chamber.

The structure of the experiment is shown in the sampling tree in figure 6. The sampling tree shows what are the variables being studied and also how the experiment was performed.

4.3 EXPERIMENTAL RESULTS

Table 4 shows the results of time to freeze the packages from 20°C to -18°C. The freezing curves of the packages at each position are shown below in figure 7.

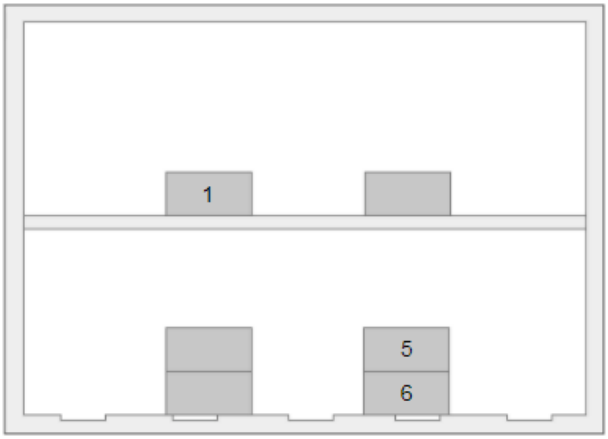

Figure 4 – Package positions set up 1 schematic. Source: Author (2020)

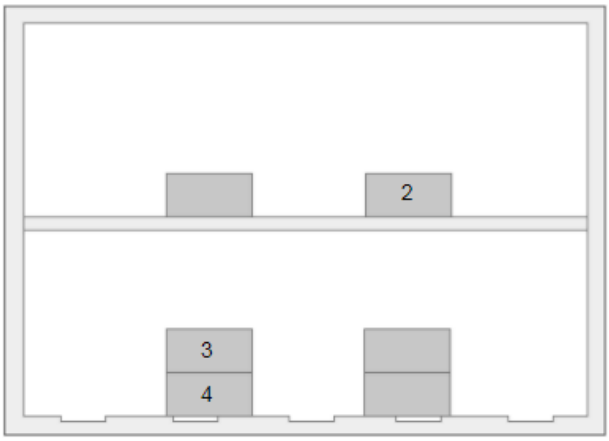

Figure 5 – Package positions set up 2 schematic. Source: Author (2020)

Table 4 – Time to freeze the packages from 20°C to -18°C in minutes. Source: Author (2020)

Refrigerator Sample	Package	Set Up	Position	Measurement 1	Measurement 2	Measurement 3
1	1	1	1	582	585	589
1	1	2	2	602	583	579
1	2	1	3	850	848	851
1	2	2	5	810	787	780
1	3	1	4	893	887	894
1	3	2	6	837	820	815
2	4	1	1	604	581	605
2	4	2	2	613	615	603
2	5	1	3	842	852	824
2	5	2	5	839	824	844
2	6	1	4	874	882	863
2	6	2	6	869	857	879

In the freezing curves it is possible to see that the phase change does not occur with a constant temperature, see figure 7. Also, it can be observed that the phase change duration varies from approximately from 2h30min to 6h depending on the position of the package inside the compartment.

4.4 STATISTICAL ANALYSIS

After the tests were finished, an analysis was performed to understand the effect of the position in the freezing time and the similarity of the packages among themselves.

The variability chart presented in figure 8 shows a systematic effect for position on the freezing time, this was expected since the airflow distribution is not uniform inside the compartment. Evaluating the results, it shows that the average freezing time is very similar between positions 1 and 2, both on the top shelf. This happens because the airflow outlets are on the region above the shelf, dedicating more intense airflow to this region. When comparing it with the results for positions 3, 4, 5 and 6 under the shelf, the freezing time is much lower. Considering these packages under the shelf, the ones located at the top of the stack (positions 3 and 5) have a slightly lower freezing time than packages in the positions 4 and 6 since they are not directly in contact with the freezer compartment surface.

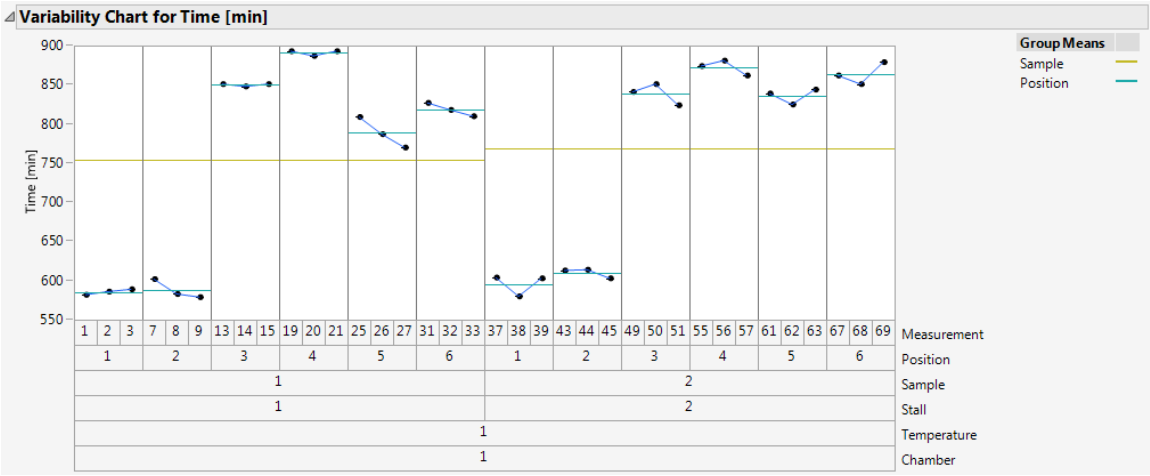

Figure 8 – Variability chart. Source: Author (2020)

In the table 5 are presented the average time of the freezing time of the tylose packages from 20°C to -18°C in the positions 1 to 6 considering the tests performed in both refrigerator samples. The estimated standard deviation (σ) calculated according to (WHEELER; LYDAY, 1989) is 11 minutes and experimental measurement uncertainty given by 2σ is 22 minutes (JR; SOUZA, 2008), this includes all the uncertainties of the experiment.

Table 5 – Experimental average freezing time from 20°C to -18°C in minutes. Source: Author (2020)

	Position 1	Position 2	Position 3	Position 4	Position 5	Position 6
$\bar{X}$	591	599	845	882	814	846

The MSE evaluation is presented in the Appendix A.

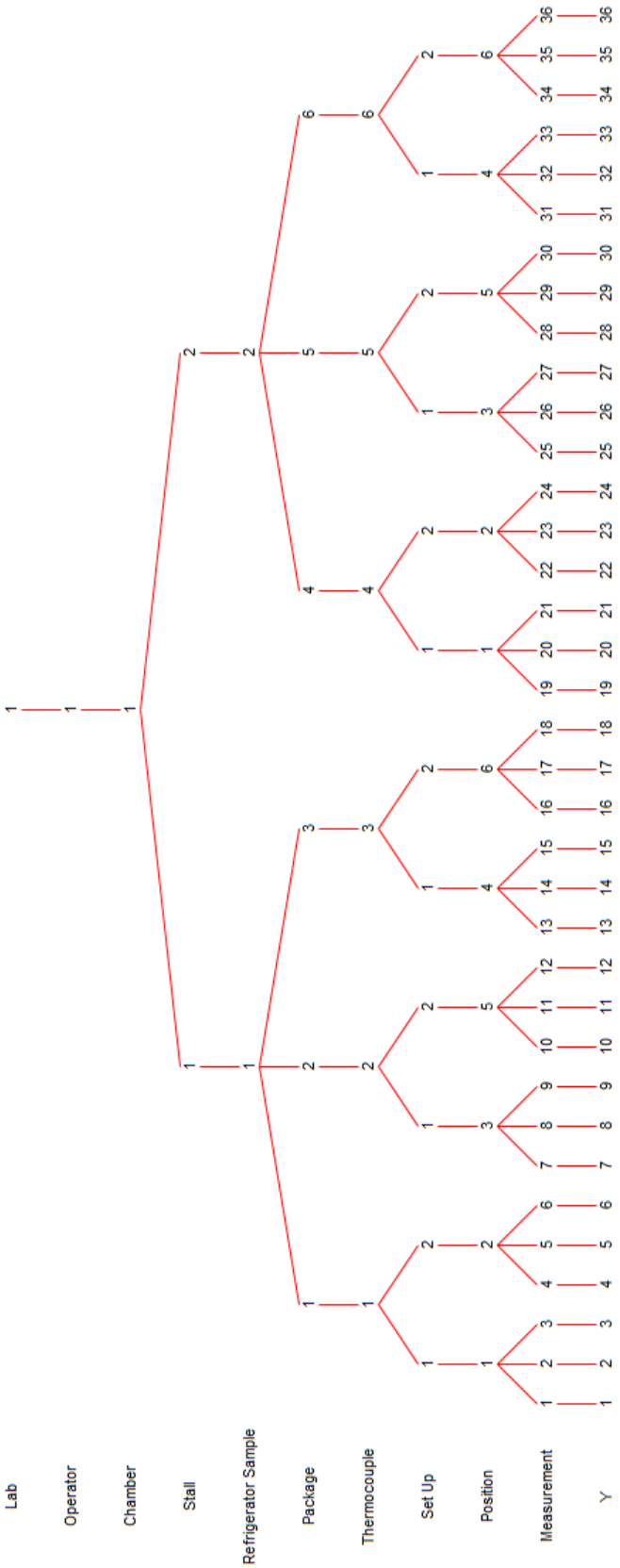

Figure 6 – Sampling Tree. Source: Author (2020)

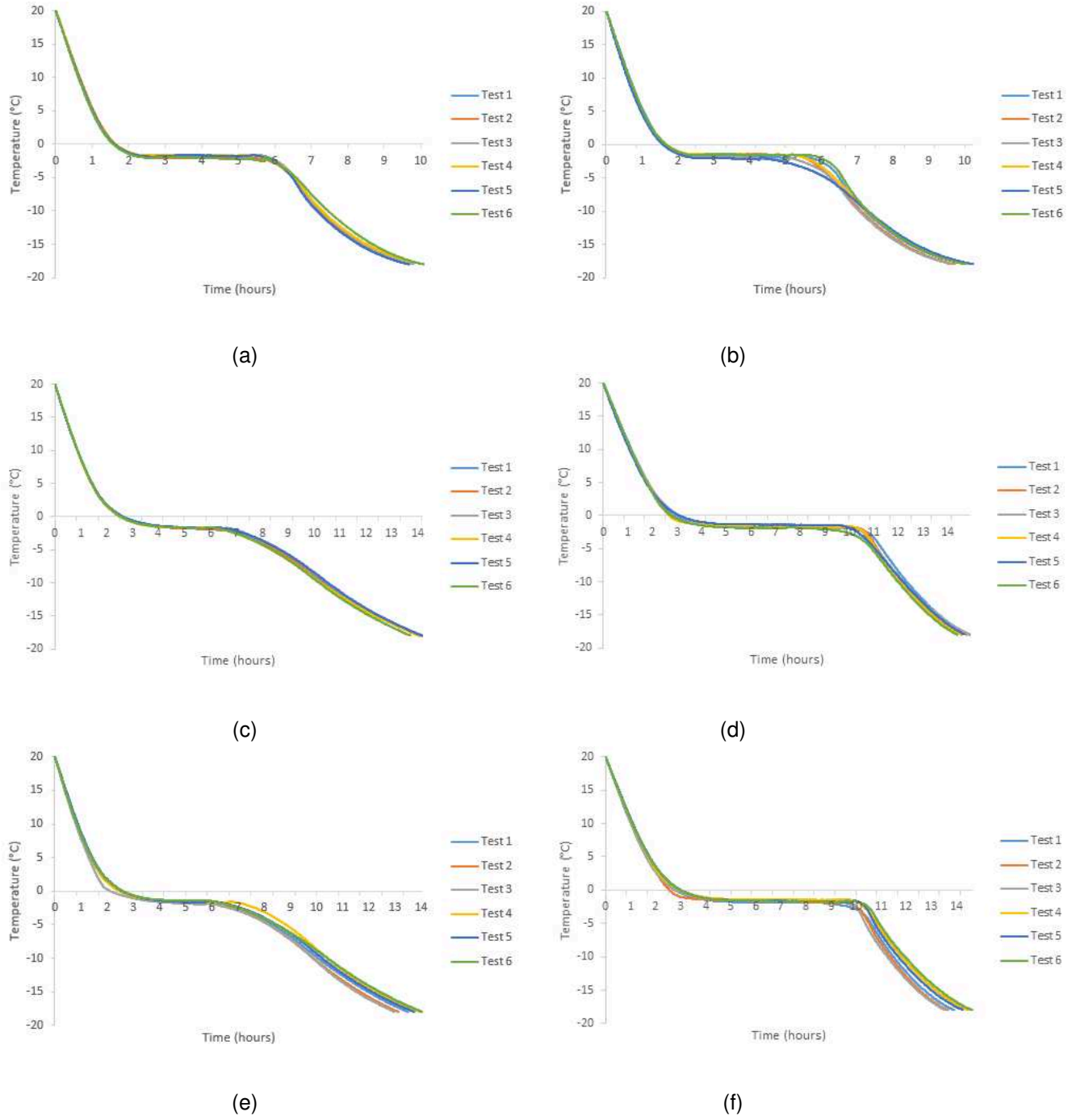

Figure 7 – Freezing curves at (a) Position 01 (b) Position 02 (c) Position 03 (d) Position 04 (e) Position 05 (f) Position 06. Source: Author (2020)

5 EQUATIONS

This chapter presents an overview of the equations used for solving the physical phenomena of the airflow inside the refrigerator with the Computer Fluid Dynamics (CFD) model applied in this study.

5.1 MATHEMATICAL EQUATIONS

The conservation laws are described below using Eulerian approach, considering a control volume and a Newtonian fluid.

5.1.1 Mass conservation

Mass conservation in a control volume is given by equation 1

$$\frac{\partial \rho}{\partial t} + \frac{\partial}{\partial x_i}(\partial u_i) = 0 \tag{1}$$

where ρ is density, t is time, u_i is the velocity vector cartesian component and x_i is the coordinate direction.

5.1.2 Momentum conservation

Momentum conservation equation in its non conservative form for Newtonian fluids is written as

$$\frac{\partial(\rho u_i)}{\partial t} + \frac{\partial \rho u_j u_i}{\partial x_j} = \frac{\partial \tau_{ij}}{\partial x_j} - \frac{\partial p}{\partial x_{ij}} + B_i \tag{2}$$

being B_i the body forces and $\tau_{ij} = \mu\left[\frac{(\partial u_i)}{(x_j)} + \frac{(\partial u_j)}{(\partial x_i)}\right] - \frac{2}{3}\mu\delta_{ij}\nabla u$ the stress tensor, where p is pressure, δ_{ij} the Kronecker delta and μ the dynamic viscosity.

5.1.3 Energy conservation

Energy conservation equation, presented in terms of total specific enthalpy, is given by 3

$$\begin{aligned}\frac{\partial(\rho h_0)}{\partial t} + \frac{\partial \rho u_i h_0}{\partial x_i} = \frac{\partial}{\partial x_i}\left(k\frac{\partial T}{\partial x_i}\right) + \frac{\partial p}{\partial t} + \left[\frac{\partial(u\tau_{xx})}{\partial x} + \frac{\partial(u\tau_{yx})}{\partial y}\right. \\ + \frac{\partial(u\tau_{zx})}{\partial z} + \frac{\partial(v\tau_{xy})}{\partial x} + \frac{\partial(v\tau_{yy})}{\partial y} + \frac{\partial(v\tau_{zy})}{\partial z} + \frac{\partial(w\tau_{xz})}{\partial x} + \frac{\partial(w\tau_{yz})}{\partial y} \\ \left. + \frac{\partial(w\tau_{zz})}{\partial z}\right] + S_h\end{aligned} \tag{3}$$

h_0 represents total specific enthalpy, defined as $h_0 = h + \frac{1}{2}(u^2 + v^2 + w^2)$. Temperature is represented by T, thermal conductivity by k and the term S_h represents the source term.

5.1.4 Equation of state

Assuming that the fluid always stays at thermodinamic equilibrium, for the flow being studied, ideal gas equation (4) is used to complete the system of equations.

$$\rho = \frac{p}{R_g T} \tag{4}$$

in which R is the specific constant of the gas.

5.2 TURBULENCE MODELLING

Turbulent flows are highly unstable and tridimensional with fluctuations in a broad size and time scale (FERZIGER; PERIC, 2002). There are different forms to model turbulence in a flow, the most accurate is called DNS - Direct Numerical Simulation, since the equations are solved without approximations. However, in order to capture all the turbulence structures the domain must be as large as the physical domain, in addition to having a refined mesh to capture the small scales where kinetic energy dissipation occurs. Thus, simulation using this method is applied for simpler geometries and with lower Reynolds number.

The LES model - Large Eddy Simulation considers that large turbulence scales have more energy than small scales, which do not have large contribution to the properties transport. In this case, the large scales are solved directly and the small scales are modeled.

However, the most applied approach for turbulence modeling is known as RANS - Reynolds-Averaged Navier-Stokes. Frequently in engineering problems the interest is in some properties that represent the flow, not needing to capture all the turbulence phenomena. In the present study the model with RANS equations is used.

In the RANS model the variables are written as the sum of the average value and as fluctuations over this value

$$\phi(x_i, y) = \bar{\phi}(x_i) + \phi'(x_i, t) \tag{5}$$

the average value is given by

$$\bar{\phi}(x_i) = \lim_{\Gamma \to \infty} \frac{1}{\Gamma} \int_0^{\Gamma} \phi(x_i, t) dt \tag{6}$$

where t is time and Γ is the interval to obtain the average, which must be large enough compared with the fluctuations time scale, as shown in figure 9. In the figure

the horizontal line represents the average value ($\bar{\phi}$), given by the integral in time interval T, and the variations around the constant line represent the fluctuations (ϕ').

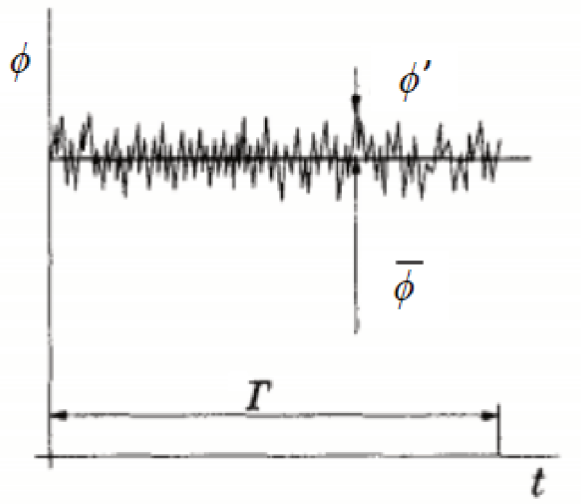

Figure 9 – Time average for a turbulent flow in steady state. Source: Adapted from (FERZIGER; PERIC, 2002)

Aplying the Reynolds averaging to the Navier-Stokes equations results in the Reyonolds Average Navier-Stokes equations (RANS). Therefore, mass conservation equation, momentum equation and energy equation for ideal gas are written, respectively, as

$$\frac{\partial(\rho\bar{u_i})}{\partial x_i} = 0 \tag{7}$$

$$\frac{\partial}{\partial x_i}(\rho\bar{u_i}\bar{u_j}) = -\frac{\partial\bar{p}}{\partial x_i} + \frac{\partial\bar{\tau_{ij}}}{\partial x_j} - \frac{\partial}{\partial x_j}(\rho\bar{u_i'u_j'}) \tag{8}$$

where

$$\bar{\tau_{ij}} = \mu\left(\frac{\partial\bar{u_i}}{\partial x_j} + \frac{\partial\bar{u_j}}{\partial x_i}\right) \tag{9}$$

Being this the strain rate tensor for average flow, and the term $-\rho\bar{u_i'u_j'}$ is known as Reynolds stress tensor.

6 NUMERICAL MODEL

In this study the numerical simulation is divided in two parts: a 3D CFD simulation and a 1D heat transfer simulation. In the CFD, the heat exchange between the air inside the refrigerator and the packages was determined and knowing the temperature difference between the air and the package surface, the UA value could be determined. The UA value was then applied as boundary condition in the 1D model to evaluate the freezing time.

Since the exact thermal properties for the tylose material were unknown, an additional step was performed. Using the tests' data and typical range values for the thermal properties an optimization process was executed to define the properties. All these steps will be discussed in the following items.

6.1 CFD MODEL

To determine the heat exchange between the package and the air inside the compartment a CFD analysis was performed using ANSYS Fluent software. The refrigerator used in the tests was modeled in a CAD software considering the packages arrangement inside the freezer compartment during the tests. Simulating the complete refrigerator with fin-on-tube evaporator resulted in a very large mesh count, due to this the simulation domain was restricted to the freezer compartment and the airflow connections between fridge and freezer compartments were considered applying boundary conditions of inlet and outlet.

For the discretization a tetrahedral mesh was defined for both surface and volumetric mesh. The objective of the CFD simulation was to evaluate the total heat flux on the surface of the packages so, in order to reduce the mesh count, the packages were defined as voids.

The boundary conditions related to the operation of the refrigerator were set based on the average values from the experimental test results and are shown in table 6 and identified in figure 10. Also, the fridge insufflation (outlet) and return (inlet) airflow rate for the fridge compartment were set as outlet and inlet boundary conditions respectively based on common known values for the product from previous simulations. The outlet value in table 6 is the gauge pressure. An adiabatic boundary condition was defined on the surfaces that were connected to the fridge compartment and a boundary condition was set in the external part of the cabinet to simulate the tested ambient condition. A temperature and convective coefficient were applied in the internal part of the evaporator tubes to simulate the refrigerant fluid flow. The packages temperature were set as a fixed temperature of -18°C since this is the minimum temperature that packages placed in the freezer need to reach in several of standard tests. The fan rotation movement was represented using a MRF model, which is a steady state approximation

in which the individual cell zones are assigned different rotational speeds and at the interface between cell zones a local reference frame transformation is executed to enable flow variables in a zone to be used to calculate fluxes at adjacent zones (ANSYS, 2019a).

Table 6 – Boundary conditions. Source: Author (2020)

Boundary condition	Value
External cabinet temperature	43°C
External cabinet convective coefficient	6 W/(m^2K)
Evaporator temperature	-28°C
Evaporator convective coefficient	3500 W/(m^2K)
Fan speed	1700 rpm
Package temperature	-18°C
Inlet mass flow rate	0.00132 Kg/s
Inlet temperature	7°C
Pressure outlet	0 Pa
Adiabatic	

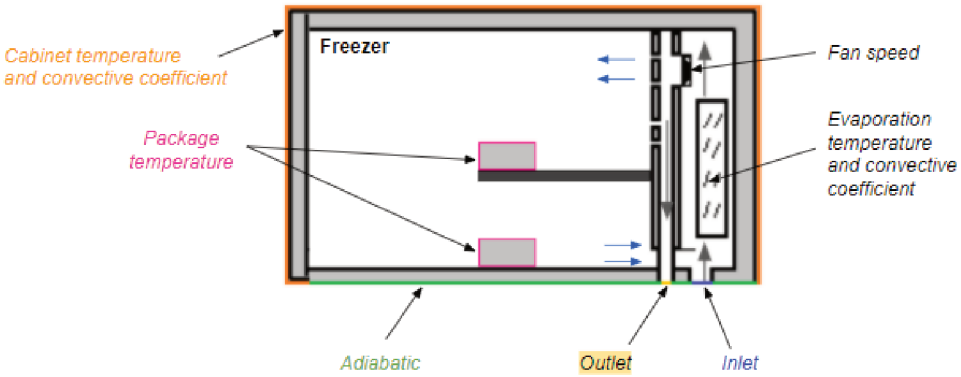

Figure 10 – Boundary conditions location. Source: Author (2020)

The airflow simulations were performed as steady state analysis. The solution method chosen was coupled, the turbulence model defined was the $k-\epsilon$ realizable and for the near wall treatment the enhanced wall treatment model was chosen (ANSYS, 2019b).

6.1.1 Mesh Refinement

A mesh size refinement study was performed considering the surface mesh in contact with the packages and the volumetric mesh of the freezer air. Four tests were performed considering the sizes shown in table 7.

Table 7 – Mesh Refinement Tests (mm). Source: Author (2020)

	Surface Mesh	Volumetric Mesh
Test 01	5	7
Test 02	4	7
Test 03	3	7
Test 04	4	6

In each of the tests it was measured the total heat transfered to the packages surfaces to evaluate the effect of the mesh sizes. The results of the integral of the total heat flux integral on each of the packages surfaces are shown in Appendix E and they show a small variation of values between the tests. The largest difference observed between Test 03 and Test 04 (which had the most refined meshes) was 5.3% in the position 01 package at the top surface. Therefore results from Test 04 were considered for the optimization and 1D heat transfer simulations.

The total heat transfer value Q at each package surface will be divided by the delta temperature ΔT between the package surface prescribed temperature and the simulated air temperature exiting the insufflation slots on the freezer plenum to define the global heat transfer coefficient UA at each surface, as shown in equation 10. The Q values were obtained calculating the integral of the total heat flux at each surface.

$$UA = \frac{Q}{\Delta T} \tag{10}$$

The UA values for each of the surfaces will be defined as input to the 1D model.

6.2 1D MODEL

The 1D model was built in the OpenModelica software, an open source Modelica-based modeling and simulation environment that contains different types of libraries such as thermal, fluids, mechanics, etc. Inside the libraries there are components that allow the modeling of different systems. Modelica is an object-oriented, equation-based, declarative language that allows acausal modelling, which is a modeling approach based on equations instead of assignments with no input and output definitions, therefore the causality is fixed as the system is solved (SCHWEIGER, 2017). A schematic of this model approach is shown in figure 11. The OpenModelica software transforms the Modelica model into an ODE representation to perform a simulation by using numerical integration methods. The DASSL solver was used in the simulations, this is a an implicit, higher order, multi-step solver being a stable solver for a large range of models (OPENMODELICA, 2020).

Three types of components were used to model the package heat transfer: a heat capacitor, a thermal conductor and a convection component. For each surface of the package there is a combination of a thermal conductor and a convection component, as

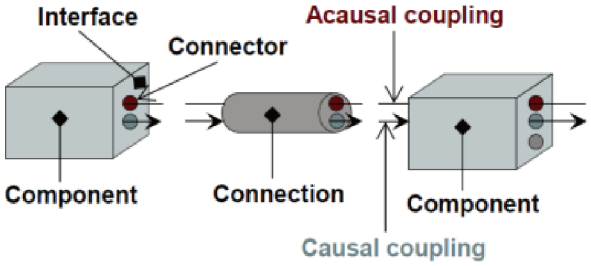

Figure 11 – Causal and acausal model approach schematic. Source: (SCHWEIGER, 2017)

shown in image 12. A fixed temperature component was used to represent the airflow average temperature measured in the tests and it was connected to the convection components of each surface. Also, P and A parameter tables were created to list the inputs for the model. In table P there are the package thermal properties (table 8) and in table A are the UA values defined in the CFD simulation (table 9).

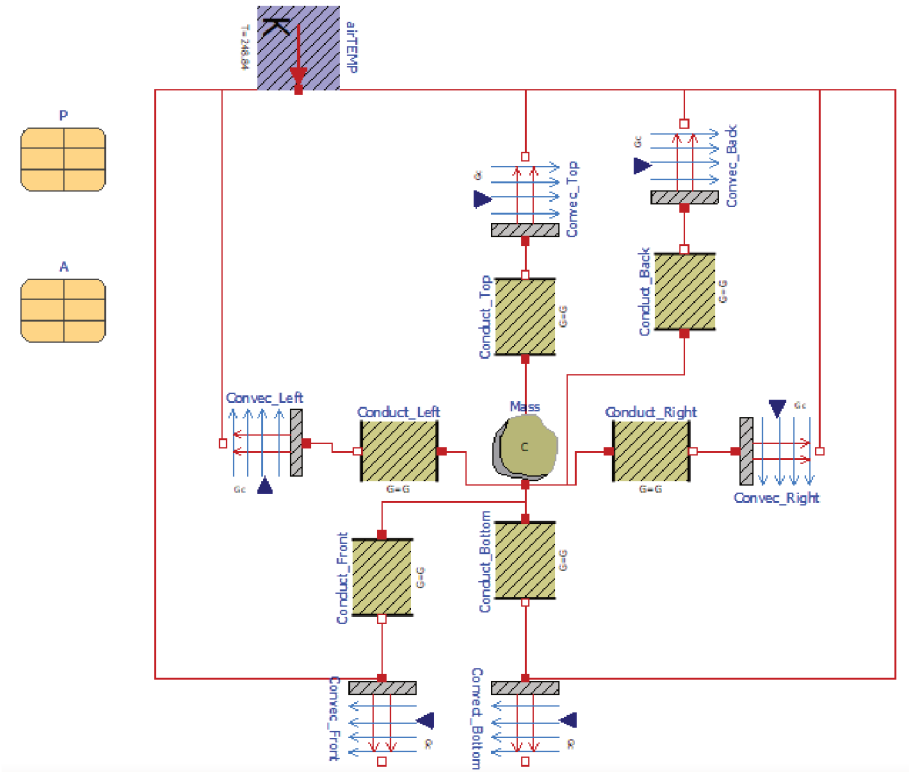

Figure 12 – Package standalone - 1D model. Source: Author (2020)

Table 8 – Parameters from table P. Source: Author (2020)

Parameter	Description
M	Mass
Tsl	Phase change temperature
DTs	Phase change temperature range
Hsl	Phase change enthalpy
Cpl	Specific heat of liquid
Cps	Specific heat of solid
kl	Thermal conductivity at liquid state
ks	Thermal conductivity at solid state

Table 9 – Parameters from table A. Source: Author (2020)

Parameter	Description
topUA	Overall heat thermal conductance - top surface
bottomUA	Overall heat thermal conductance - bottom surface
frontUA	Overall heat thermal conductance - front surface
backUA	Overall heat thermal conductance - back surface
leftUA	Overall heat thermal conductance - left surface
rightUA	Overall heat thermal conductance - right surface

The thermal capacitor element represented as Mass in the center of figure 12 has the following inputs from table P: M, Tsl, Dts, Hsl, Cpl and Cps. Also, in this component it is set the element initialization temperature, which in this study is 20°C. The thermal conductor elements receive the table P inputs: kl, ks, Tsl and DTs. Also, for each element is defined the surface area A and the distance L from the center to surface of the package. For the convective element the input is the UA value defined in the CFD simulation. An identical model was constructed for the packages stacked and is shown in figure 13 (packages in positions 3, 4, 5 and 6).

Since the tylose is a phase change material, the thermal capacitor and the thermal conductor elements had conditional equations applied to them so the appropriate thermal properties were applied depending on the phase that the material was in during the simulation. The equations applied in the elements are shown below.

The heat transfer for the conductivity element is

$$Q = \frac{kA(T_c - T_{surf})}{L} \tag{11}$$

where T_c is the temperature at the center of the package, T_{surf} is the temperature of the package surface and k varies depending on the state, being k_s for the solid state, k_l for the liquid state and in the phase change state it is an intermediate value depending on the fraction of liquid.

Convective heat transfer is given by

$$Q = UA(T_{surf} - T_a) \tag{12}$$

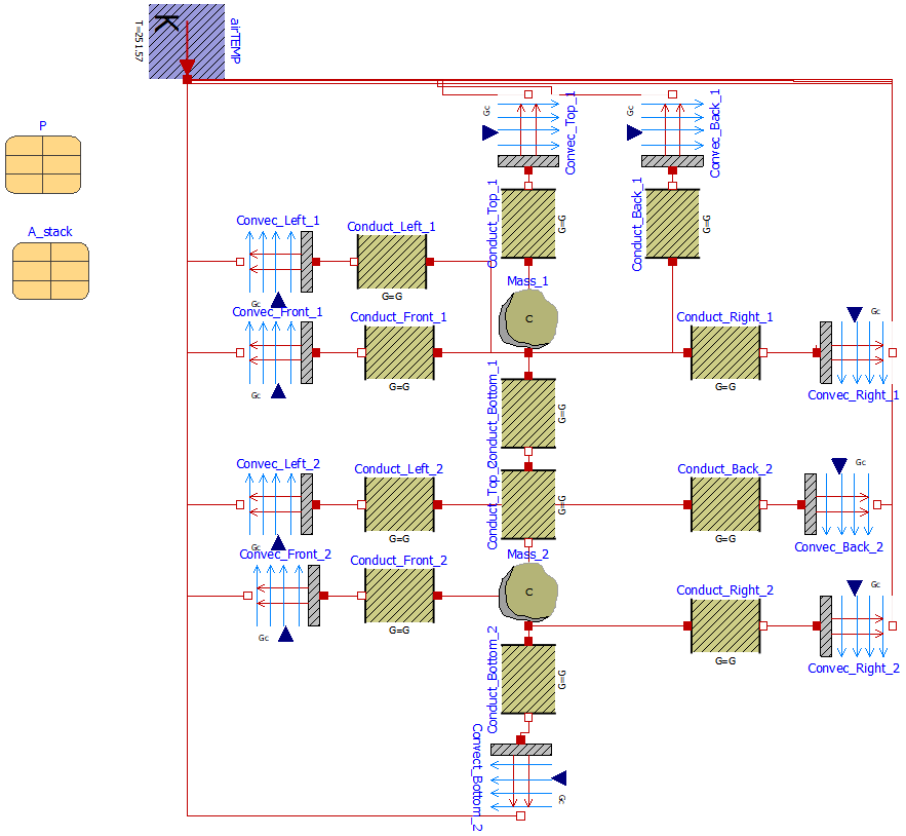

Figure 13 – Packages stacked - 1D model. Source: Author (2020)

where T_{surf} is the temperature of the package surface and T_a is the temperature of the air.

The thermal energy equation is,

$$Q = MCp\frac{dT}{dt} \tag{13}$$

M is the mass, dT/dt is the time derivative of temperature. The Cp value varies at each stage of the solidification process, so there is a Cp for the solid, for the liquid and for the phase change region. An adaptation of the enthalpy method (MACHNIEWICZ; HEIM, 2014) was applied to model the phase change portion of the curve as shown in figure 14.

For a material under constant pressure with small volume changes, the Cp can be written as in equation 14. In the modeling approach used, dH is the enthalpy difference between the liquid and solid phase and dT is the temperature variation along this phase, represented by the variables Hsl and DTs in the problem as shown in figure 15.

$$Cp = \frac{dH}{dT} \tag{14}$$

The equations modelled in OpenModelica are described in Appendix B, C and D, and were applied to all components. Besides the properties that were already defined

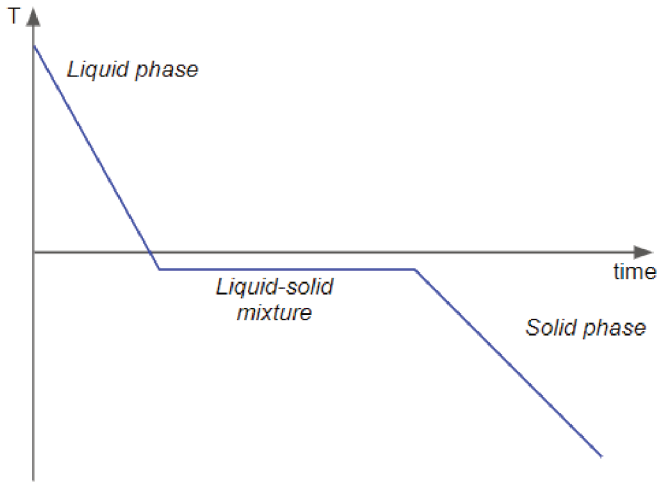

Figure 14 – Phase change curve scheme. Source: Author (2020)

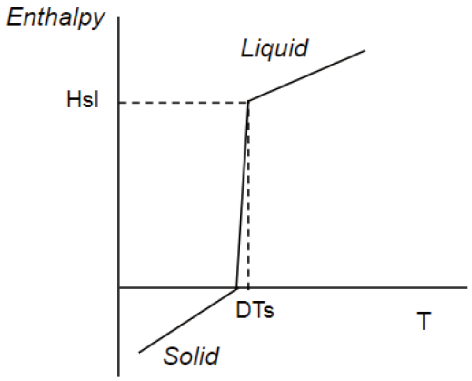

Figure 15 – Enthalpy curve scheme. Source: Author (2020)

in table 8, some additional variables were included in the code. In order to have the appropriate thermal conduction factor k for each phase and during the phase change, a variable fs was defined to evaluate the fraction of liquid existing during the simulation and it is given by

$$fs = \frac{T - (Tsl - 0.5DTs)}{DTs} \tag{15}$$

6.3 OPTIMIZATION MODEL

The thermal properties of the tylose packages used in the experimental tests were unknown, only some values from the literature were available. In order to have the values that represent correctly the properties and therefore could be used to estimate the time to freeze of each package, an optimization was performed.

The optimization was performed in the software ModeFrontier and consisted in identifying the optimum values for the thermal properties within a defined range for each of the variables that would result in a smaller difference between the points on the

experimental and simulated freezing curves for the same points in time. The packages considered in the optimization were in the positions 01, 05 and 06 (figure 4) and for each time defined it was taken the average temperature of the six experimental tests, considering refrigerator samples 01 and 02. Only three out of the total six packages were used so that the other three could be applied in the validation. The values are detailed in table 10. The standard deviation was calculated splitting the values into temperature subsets: values higher than 0°C, values between 0°C and -2.5°C and values lower than -2.5°C, the details of the analysis are show in Appendix E. For the values higher than 0°C the standard deviation is 0.3°C and the experimental measurement uncertainty is 0.6°C, for the range between 0°C and -2.5°C the standard deviation and experimental measurement uncertainty are respectively 0.2 °C and 0.4°C, then for values lower than -2.5°C the standard deviation is 0.5°C and the experimental measurement uncertainty is 1.0°C.

Table 10 – Average temperature at time intervals for packages at positions 01, 05 and 06. Source: Author (2020)

Time (min)	Position 01 (°C)	Position 02 (°C)	Position 03 (°C)
30	12.1	13.9	15.2
60	5.1	8.4	10.5
90	0.6	4.1	6.4
120	-1.3	1.3	3.1
180	-1.8	-0.8	-0.3
240	-1.8	-1.4	-1.3
300	-1.9	-1.6	-1.5
360	-2.6	-1.6	-1.6
420	-8.5	-2.5	-1.6
480	-13.4	-1.4	-1.7
540	-16.5	-6.5	-1.8
600	-17.9	-9.6	-2.2
660	-	-12.5	-7.0
720	-	-15.0	-11.8
780	-	-16.9	-15.4

Ranges for all the thermal properties were also defined as inputs to define the inference space for the optimization process and they are listed in table 11. The ranges were defined considering the test results and some literature information available, also a wider range was considered for most of the cases so the solution would be reaching the lower and upper ranges for all the parameters.

Table 11 – Thermal properties ranges for optimization. Source: Author (2020)

Parameter	Lower Range	Upper Range	Unit
Tsl	-1	-2.5	°C
Dts	0.5	1.0	°C
Hsl	100000	334000	J/Kg°C
Cpl	2000	5000	J/Kg°C
Cps	1000	4000	J/Kg°C
kl	0.15	0.6	W/mK
ks	0.7	2.0	W/mK

The optimization algorithm used was the pilOPT, a multi-strategy self adapting algorithm (MODEFRONTIER, 2019). The objective function was set to minimize the sum of squares of the difference between the simulated and experimental temperature for standalone package as defined in the equation below

$$Objective = \sum_{w=1}^{n} (T_{sim_w} - T_{exp_w})^2 \tag{16}$$

where n is the number of points of the packages in the positions 01, 05 and 06 defined in the table 10. The optimizations runned 5000 iterations each.

7 RESULTS

In this chapter it will be presented the results obtained with the numerical models and the comparison with the experimental data. They are divided in three sections: first section shows the global heat transfer coefficients obtained from the CFD simulation, the second section presents the material properties values results obtained through the optimization and the last section shows the comparison of numerical and experimental freezing curves and times.

7.1 GLOBAL HEAT TRANSFER COEFFICIENTS

The global heat transfer coefficients UA of each package surface was calculated using equation 10 considering the packages surface heat transfer of Test 04 from tables 17 to 22 in Appendix F and the ΔT of 5.72K, measured in the CFD simulation.

Table 12 shows the UA values at each surface considering a front view from the freezer compartment. The packages numbers are references of the positions shown in figures 4 and 5. The surfaces that have contact between packages (packages in positions 3-4 and 5-6) in the stacks are not present in table 12. The temperature on the geometric center above and under the shelf was also measured in the simulation and the results along with the experimental values are shown in table 13.

Table 12 – UA values (W/K). Source: Author (2020)

	Top	Right	Left	Front	Bottom	Back
Position 01	0.05960	0.03521	0.02953	0.04332	0.06142	0.04210
Position 02	0.06744	0.02729	0.05249	0.03604	0.05633	0.03034
Position 03	0.08348	0.03848	0.03093	0.05399	-	0.02198
Position 04	-	0.02996	0.02157	0.04660	0.02004	0.01693
Position 05	0.06360	0.02045	0.03912	0.03580	-	0.02461
Position 06	-	0.01954	0.04056	0.03740	0.01495	0.02038

The results in the table 12 show larger UA values for most of the top surface of the packages. This happens due to the airflow pattern inside the compartment, the system insufflates air at the top of the compartment, where packages in the positions 01 and 02 were located, and returns under the shelf at the bottom of the plenum where packages in the positions 03 to 06 were placed. Bottom surface of packages in the positions 04 and 06 have a smaller UA value compared to packages in the positions 01 and 02 because they are placed at the floor of the freezer compartment, having a small air passage to extract heat, differently from the bottom surfaces of packages 01 and 02 that have higher UA values at this surface since the air flows under the shelf where they are placed allowing more heat to be exchanged. Since there is no preferential direction inside the compartment the values for the surfaces can vary at each position.

Table 13 – Air temperature (°C) at the geometric center above (Freezer position 1) and under (Freezer position 2) the shelf in freezer compartment. Source: Author (2020)

	Freezer position 1	Freezer position 2
Exp Test 01	-22.2	-21.5
Exp Test 02	-22.6	-21.8
Exp Test 03	-22.6	-21.8
Exp Test 04	-22.7	-21.9
Exp Test 05	-22.6	-21.8
Exp Test 06	-22.7	-21.8
Exp Test 07	-21.7	-21.1
Exp Test 08	-22.1	-21.5
Exp Test 09	-22.1	-21.6
Exp Test 10	-22.4	-21.6
Exp Test 11	-22.3	-21.7
Exp Test 12	-22.5	-21.9
$\bar{X}$	-22.4	-21.7
Simulation	-22.6	-22.17

The experimental results are presented in table 13 show the temperature of the air in the two positions inside the freezer compartment. The standard deviation for the measurements is 0.2°C and the total experimental measurement uncertainty is 0.4°C considering the sample tree in Appendix G. The data show a good correlation between the CFD simulation performed and the experimental tests results for the air temperature measured inside the freezer compartment.

7.2 FREEZING CURVES

The UA values for the packages 01, 05 and 06 positions presented in table 12 were defined as inputs in the 1D model presented in section 6.2 and the optimization was performed as described in section 6.3.

The first optimization performed targeted to find the thermal properties that would ensure the minimum value of the objective function (equation 16) for the packages in the three positions simultaneously. In order to do it the individual objective functions were summed as shown in equation below.

$$Objective_{Sum} = Objective_{Pos01} + Objective_{Pos05} + Objective_{Pos06} \tag{17}$$

In this first optimization, the staked 1D model was built not considering any thermal resistance between the bottom and top surfaces. The results for the packages freezing curves at the positions 01, 05 and 06 are shown in the figure 16. In figure 16b it can be observed an unexpected behavior in the solid part of the freezing curve of package in position 05, showing a step at the approximately same time as the package

in position 06 exits the solid-liquid mixture region phase of the curve and starts the solid phase. This issue occurred because of a modeling artifice used in the below

$$T = \frac{Ta + Tb}{2} \tag{18}$$

Since there is only one thermal conductor element between the center and the surface of the package the strategy chosen to capture the best way possible an intermediate temperature between those points, and therefore define the thermal conductivity, was to use an average of the center and the surface temperature. This is done with an average of the ports as shown below

This approach provides a good estimation for a standalone package but when a connection between two different packages is considered, the surface temperature of the packages starts to influence one another. So in order to mitigate this effect on the stacked packages a thermal resistance conductor was placed between the two stacked packages.

The 1D model considering the thermal resistance conductor between upper and lower packages in the stack is shown in Figure 17. The thermal resistance value was defined considering the following equation

$$G = \frac{k_r A_r}{L_r} \tag{19}$$

For the thermal conductivity k_r it was considered a plastic average thermal conductivity of 0.15 W/mK since the packages are involved in a plastic wrapping in order to maintain the rectangular shape specified in the table 2. The area A_r considered was 0.01 m², which is the contact area between both packages, and for the length L_r it was defined the value of 0.002 m, considering that each of the packages have a plastic wrapping thickness of 1 mm.

The next optimization considered the model with the thermal resistance in the stacked model and two tests were performed to understand which one would provide better results:

1. Minimize the objective function for the packages in positions 01, 05 and 06 simultaneously considering the equation 17

2. Minimize the objective function considering only the standalone package in the position 01 with the equation 16

The results of the packages freezing curve considering the thermal properties obtained with the first test mentioned above are shown in figure 18. Evaluating the freezing curves it can be noticed that the liquid phase seems to have a good correlation between experimental and simulated results for all the package positions. However

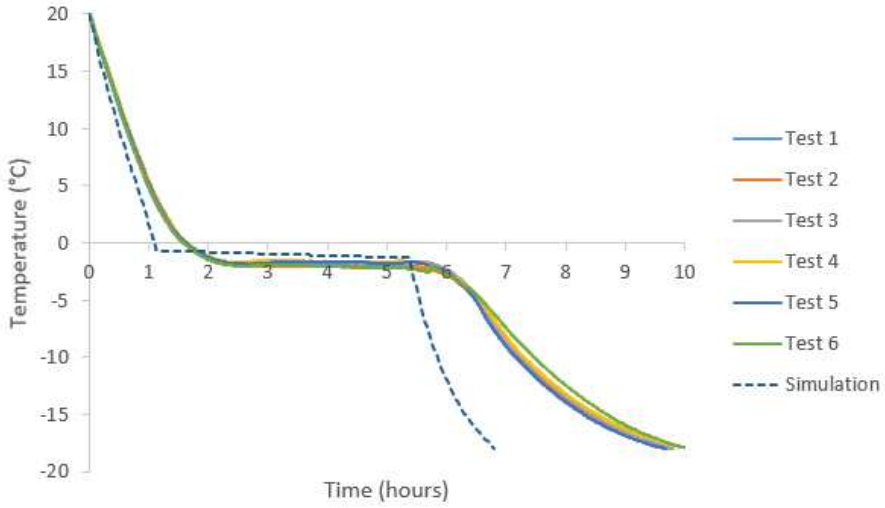

(a)

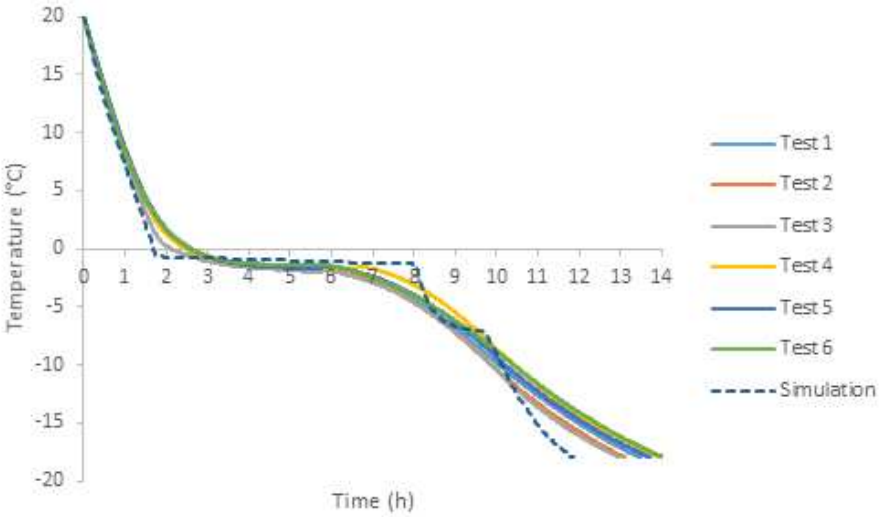

(b)

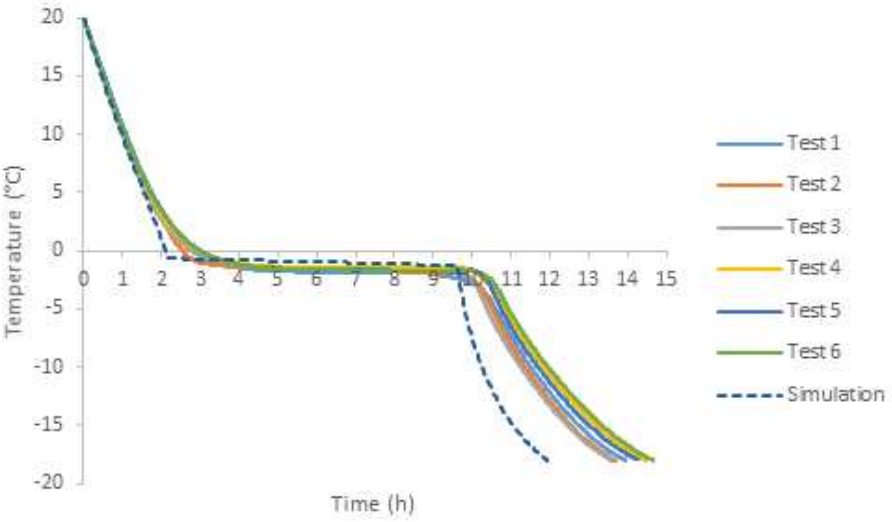

(c)

Figure 16 – Model without thermal resistance - Optimization results for packages at (a) Position 01 (b) Position 05 (c) Position 06. Source: Author (2020)

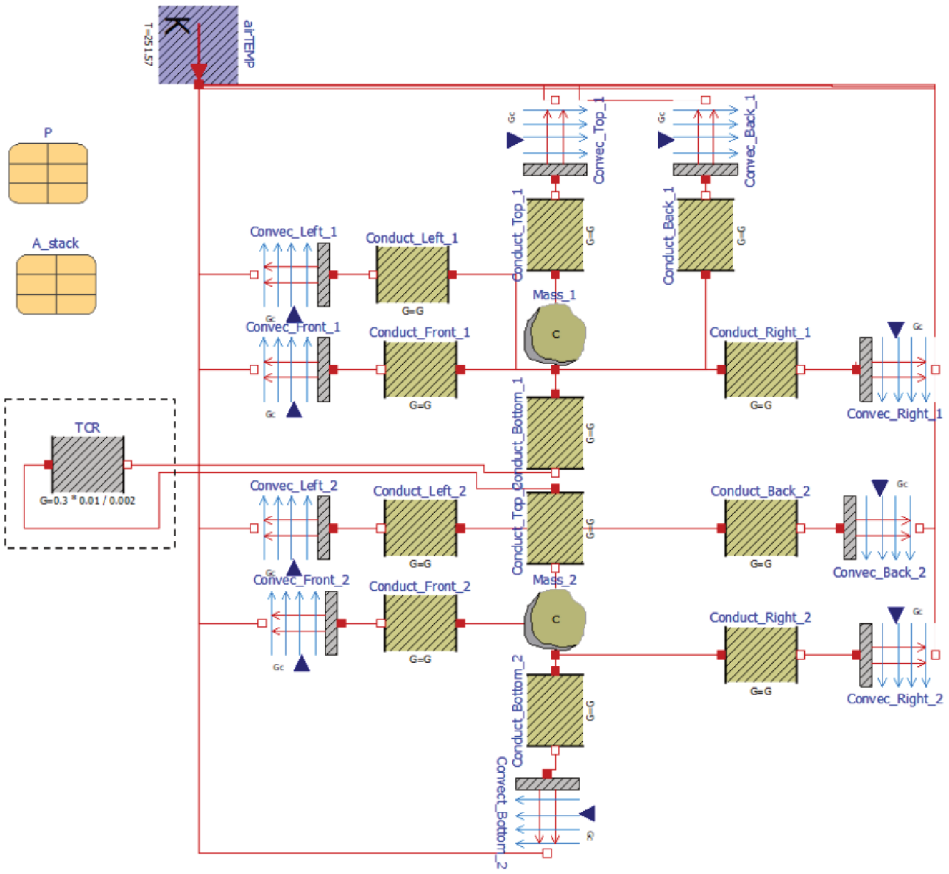

Figure 17 – Packages stacked with thermal resistance conductor - 1D Model. Source: Author (2020)

the solid-liquid mixture and solid phases of the simulated curves do not have a good correlation with the experimental pattern and time results.

The closest simulated result is the package in the position 05, where the phase change portion ends at a time close to the experimental and the solid portion is adhering better to the experimental curves. Since the optimization was performed considering the packages in positions 01, 05 and 06 it is possible that the lower value for results obtained from equation 17 was mainly driven by position 05 results.

A possible coincidence in the results for the packages in the positions 03 and 04 (figures 18c and 18d) is that even though the freezing curve is not correctly represented in the liquid-solid mixture and solid portion the simulated freezing time seems to be close to the experimental value.

The second optimization test considered only the standalone package 01 to search for the optimal thermophysical properties. The results of the packages freezing curve using these thermal properties are shown in the figure 19. For these results we can also see the good correlation between the experimental and simulated results in the liquid portion of the curves, being sightly better in the packages at the positions 01 to 04.

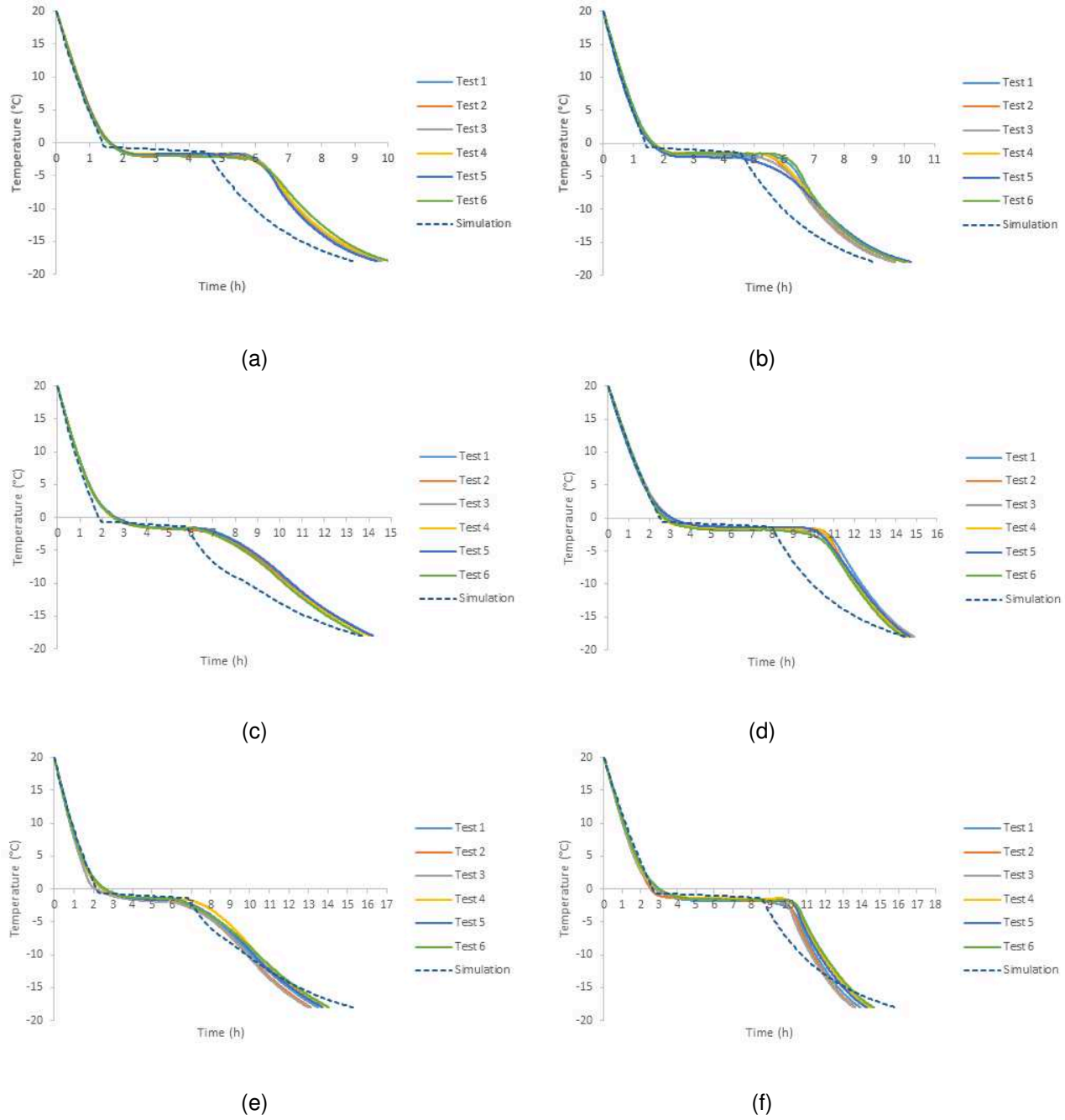

Figure 18 – Model with thermal properties from optimization of three packages - Freezing curves at (a) Position 01 (b) Position 02 (c) Position 03 (d) Position 04 (e) Position 05 (f) Position 06. Source: Author (2020)

Evaluating the results from the standalone packages in the positions 01 and 02 (figures 19a and 19b) we can observe a good agreement in terms of curves profile and each phase duration between the experimental and simulated curves and, consequently, in the total freezing time of the packages.

On the other side, the results of the packages on the stack did not have a great agreement between experimental and simulation data. Simulation results for the packages in the positions 04 and 06 (figures 19d and 19f), located in the bottom of the

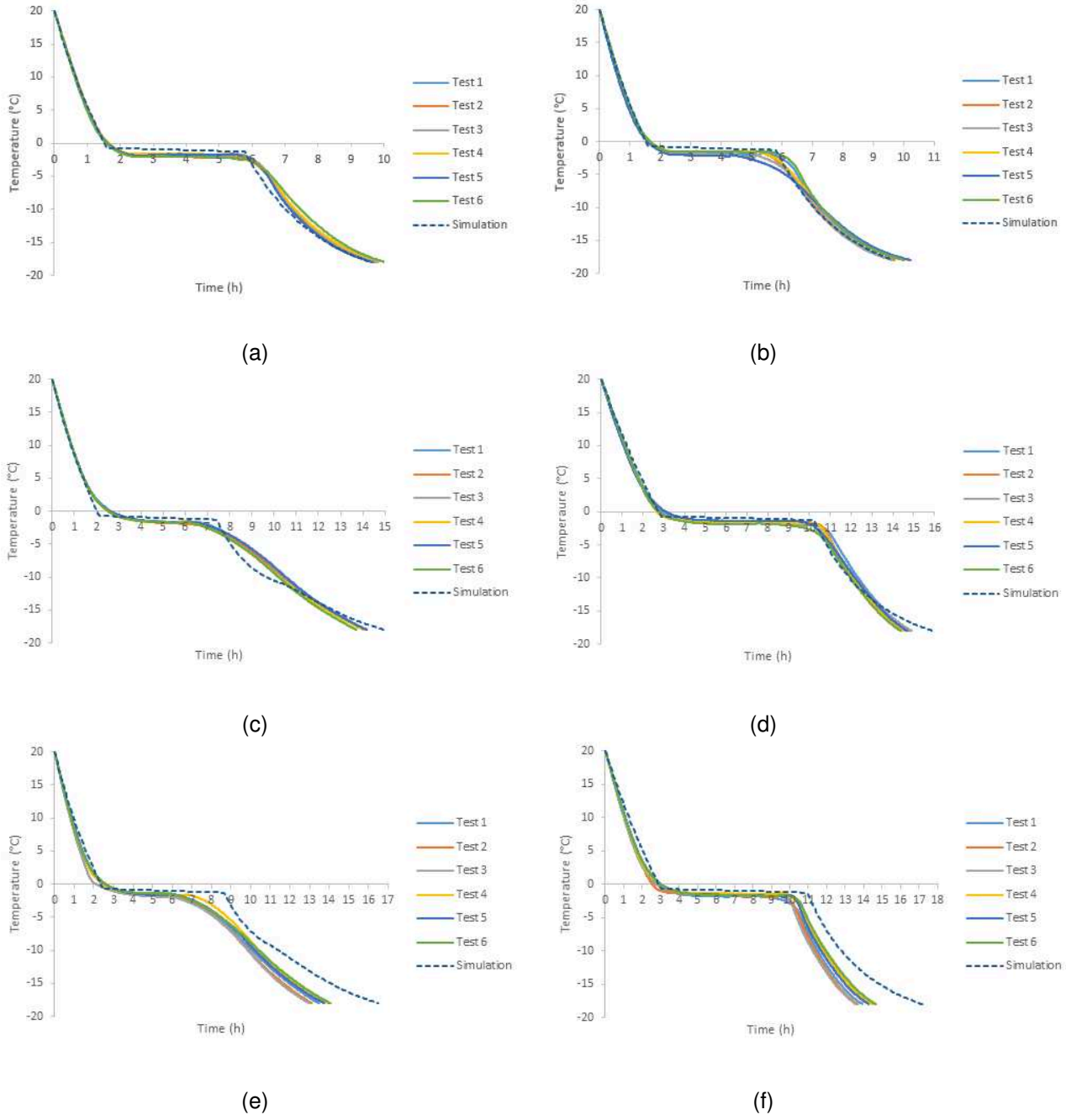

Figure 19 – Model with thermal properties from optimization of standalone package - Freezing curves at (a) Position 01 (b) Position 02 (c) Position 03 (d) Position 04 (e) Position 05 (f) Position 06. Source: Author (2020)

stack, seem to have a good prediction of the shape of the curve on the solid portion but are not able to correctly predict the time of the phases. The difference might happen due to any interaction between the packages and the freezer floor that was not captured in the model or was over simplified.

The packages in the positions 03 and 05 (figures 19c and 19e), located in the top of the stack, did not have a good correlation of the simulated curve, in the phase change and the solid portion. Looking at the experimental curves it can be observed

that they do not behave like the curves from the packages in the other positions where after the almost flat phase change portion there is a clear change in the angle when the solid portion starts, differently from these packages in the positions 03 and 05 where there is a a very smooth transition occurring. Considering the effect seen in the model without the thermal resistance it is possible that the packages on the bottom of the stack influence this portion of the freezing curve and the model was not able to predict this effect.

7.3 FREEZING TIMES

The results of both optimizations, the three packages simultaneously and the standalone package, were also evaluated in terms of the total freezing time considering the start at 20°C and the end at -18°C. In table 14 are presented the experimental total freezing time for the packages in each position and the simulated results, where simulation 1 is with the thermal properties defined in the optimization with minimum objective for the three packages and simulation 2 is for the standalone package. Remembering that for the optimization the average of the six tests performed for each position was considered.

Considering the values from table 14 it is possible to confirm the points highlighted in the previous section. The results for simulation 2, with the thermal properties obtained with the package standalone, provided a good adherence to the average experimental freezing time for the packages in the positions 01 and 02 with variation of -2.4% and -3.2%. However a larger difference is observed in the other positions for the stacked packages, which reinforces the need to better understand the modeling of the stack. The results from simulation 1 also confirm the analysis done on the previous section, even though the simulated total freezing times do not seem to be so far from the experimental values, the curves were not representative of the real behavior of the package freezing.

Table 14 – Total freezing time. Source: Author (2020)

	Position 01	Position 02	Position 03	Position 04	Position 05	Position 06
Exp Test 01	9h42min	10h01min	14h10min	14h53min	13h29min	13h56min
Exp Test 02	9h45min	9h43min	14h07min	14h47min	13h07min	13h40min
Exp Test 03	9h49min	9h38min	14h11min	14h54min	12h59min	13h35min
Exp Test 04	10h04min	10h13min	14h02min	14h34min	13h59min	14h28min
Exp Test 05	9h40min	10h14min	14h11min	14h42min	13h44min	14h17min
Exp Test 06	10h04min	10h02min	13h43min	14h23min	14h03min	14h39min
$\bar{X}$	9h50min	9h58min	14h04min	14h42min	13h33min	14h06min
Simulation 1	8h56min	9h00min	13h41min	14h29min	15h15min	15h47min
Difference	-9.3%	-9.9%	-2.7%	-1.5%	12.4%	11.9%
Simulation 2	9h37min	9h40min	14h55min	15h52min	16h30min	17h8min
Difference	-2.4%	-3.2%	6.0%	7.9%	21.6%	21.5%

7.4 THERMAL PROPERTIES

Based on the results presented in the previous sections it is correct to say that the thermal properties definition should not be based only on the total time to freeze the tylose package but also on the behavior of the freezing curve. Therefore considering both time and curve behavior we can say that the thermophysical properties that deliver the best results considering a standalone package are the ones obtained from the optimization that aimed minimize the objective function for a standalone package. In the table 15 are listed the properties from this optimization.

Table 15 – Optimized thermophysical properties. Source: Author (2020)

Parameter	Description
Tsl	-1°C
DTs	0.57°C
Hsl	123860 J/Kg
Cpl	3059.9 J/KgK
Cps	3187.6 J/KgK
kl	0.523 W/mK
ks	0.738 W/mK

Comparing the values obtained in the optimization with the ones from table 1, it can be observed that the phase change enthalpy is not the same but presents a value in a close range from the literature. For the specific heat there is a different behaviour, in the optimized results the Cps has a higher value than the Cpl which is the opposite from the literature numbers. For the thermal conductivity, the kl presents a value within the literature values, however the ks presents a lower number than the ones found in the literature. Regarding the phase change temperature, the value is different since the packages tested had a specified phase change temperature of -1°C.

8 CONCLUSION

8.1 FINAL CONCLUSIONS

For refrigerator appliances being able to correctly predict the freezing time of the stored items is very important for both food preservation and energy consumption. Being effective in the airflow flow design allows the most efficient use of the energy, which has been targeted by many countries through the release of new energy regulations reducing the targets for energy classes. This requires the manufacturers of home appliances to design more efficient systems.

In the industry, testing is a very important stage of the product development, being used to validate the product in terms of design and manufacturing, however it requires prototypes building for the tests, which may not be the best solution at early stages of the development where the design concepts are not defined yet. For the early stages of the product development simulation is a very useful tool to validate or not concepts. The present work aimed to develop a simulation model that could be used in the industry where both time and accuracy are important factors.

This study proposed a numerical method combining the application of a CFD model, a 1D model and an optimization model to predict the freezing curve and time of tylose packages. In order to have correlation data to validate the model, experimental tests were performed.

The experimental tests were performed with no-frost household refrigerators, which were loaded with tylose packages at predefined positions inside the freezer compartment and tested in a controlled chamber. Using a commercial product instead of a laboratory equipment to perform the test could generate a larger variation in the results since it is more difficult to control any product manufacturing variation that may happen, however the results showed a good consistency between the two refrigerator samples used in the tests.

The simulation method proposed consisted in the combination of three different models. The CFD model was used to define the heat transfer in each of the packages surfaces through the simulation of the airflow inside the freezer compartment. This simulation also provided the average temperature of the air exiting the insufflation slots of the compartment, which was used in the calculation of the delta temperature between the air and package surface temperature. The values for heat transfer and delta temperature allowed the calculation of global heat transfer coefficients UA for the packages surface at each of the positions which are inputs for the 1D model. A mesh refinement study was performed to define the best relationship between mesh count and output values. The results presented a small variation considering all the tests and the model with the smaller volume mesh size was chosen.

In the 1D model the global heat transfer coefficient was used in the convective

heat transfer equations, not requiring to calculate the convective coefficient h, which usually is a more difficult number to obtain. The conduction heat transfer and the thermal capacitance were also modeled and customized for the both standalone and stacked packages being able to deliver a phase change curve in the simulation.

With the results of the CFD and the 1D models the optimization was performed to define the thermophysical properties that best represented the material considering the experimental results. The first optimization showed an unexpected behavior in the curve of the package in top of the stack, showing a large influence of the temperature of the package in the bottom of the stack, therefore a thermal resistance was implemented in the 1D model for the stacked packages. The second round of optimization targeted to minimize the objective function considering the data for three packages, one standalone and two stacked, and only for a standalone package. The results considering the thermophysical properties from the optimization with three packages showed a bad correlation between the experimental and simulated curves, especially in the phase change and solid phases of the curve. On the other hand, good results were obtained with the thermophysical properties from the optimization with a standalone package, which are Tsl = -1°C, DTs = 0.57°C, Hsl = 123860 J/Kg, Cps = 3059.9 J/KgK, Cps = 3187.6 J/KgK, kl = 0.523 W/mK and ks = 0.738 W/mK. There was a good agreement between the experimental and simulated curves and the freezing times for both standalone packages with difference of -2.4% and -3.2% between simulated and experimental results, however for the stacked packages the difference was up to 21.6% between experimental and simulated results.

The simulation approach, the 1D model developed and thermal properties defined are able to predict the freezing curve and the total freezing time of a standalone package with a smaller time and computational effort than a transient CFD simulation. For the stacked packages, the 1D model considerations need to be reviewed, some of the interactions that occur in the physical arrangement were not properly modeled such as the contact between the package and the freezer floor.

8.2 SUGGESTION FOR FUTURE WORK

- Improvement of the 1D model for the stacked packages working in solutions to better model the contacts between surfaces.
- The simulation approach can be expanded and be applied in different material submitted to a freezing process.
- Evaluation of a more discretized domain in terms of conductor elements to understand if there is improvement in the correlation with experimental curves.
- CFD transient simulation to compare the results.

- Improvement of the experimental results.

REFERÊNCIAS

ANSYS. **Fluent Theory Guide Version 2019 R2**. [S.l.: s.n.], 2019.

ANSYS. **Fluent User Guide Version 2019 R2**. [S.l.: s.n.], 2019.

BECKER, B.R.; FRICKE, B.A. Freezing times of regularly shaped food items. **International Communications in Heat and Mass Transfer**, v. 26, p. 617–626, 1999.

CASTRO-GIRÁLDEZ, M. et al. Thermodynamic approach of meat freezing process. **Innovative Food Science and Emerging Technologies**, v. 23, p. 138–145, 2014.

CLELAND, A. C.; EARLE, R. L. Assessment of freezing time prediction methods. **Journal of Food Science**, v. 49, p. 1034–1042, 1984.

CLELAND, D. J. Prediction of freezing and thawing times for foods. Massey University, 1985.

FERZIGER, J. H.; PERIC, M. **Computational methods for fluid dynamics**. [S.l.]: Springer, 2002.

HOSSAIM, Md.M.; CLELAND, D.J.; CLELAND, A.C. Prediction of freezing and thawing times for foods of regular multi-dimensional shape by using an analytically derived geometric factor. **Int. J. Refrig.**, v. 15, p. 227–234, 1992.

HU, Z.; SUN, D. Predicting local surface heat transfer coefficients by different turbulent $k - \epsilon$ models to simulate heat and moisture transfer during air-blast chilling. **International Journal of Refrigeration**, v. 24, p. 702–717, 2001.

ICIER, F; ILICALI, C. The use of tylose as a food analog in ohmic heating studies. **Journal of Food Engineering**, v. 31, p. 1013–1020, 2005.

JR, A. A. G.; SOUZA, A. R. **Fundamentos da metrologia científica e industrial**. [S.l.]: Manole, 2008.

LLAVE, Y et al. Dielectric properties and model food application of tylose water pastes during microwave thawing and heating. **Journal of Food Engineering**, v. 69, p. 67–77, 2016.

MACHNIEWICZ, a.; HEIM, D. Modelling of latent heat storage in PCM modified components. **Technical Transactions Civil Engineering**, v. 19, p. 161–167, 2014.

MODEFRONTIER. **ModeFRONTIER User Guide**. [S.l.: s.n.], 2019. Accessed: November 23, 2020.

MULOT, V. et al. Measurement of food dehydration during freezing in mechanical and cryogenic freezing conditions. **International Journal of Refrigeration**, v. 103, p. 329–338, 2019.

OPENMODELICA. **OpenModelica User Guide**. [S.l.: s.n.], 2020. `https://www.openmodelica.org/doc/OpenModelicaUsersGuide/latest/`. Accessed: November 23, 2020.

OTERO, L et al. Evaluation of the thermophysical properties of tylose gel under pressure in the phase change domain. **Food Hydrocolloids**, v. 20, p. 449–460, 2006.

PHAM, Q.T. Analytical method for predicting freezing times of rectanguler blocks of foodstuffs. **International Journal of Refrigeration**, v. 8, p. 43–47, 1985.

PHAM, Q.T.; TRUJILLO, F.J.; MCPHAIL, N. Finite element model for beef chilling using CFD-generated heat transfer coefficients. **International Journal of Refrigeration**, v. 32, p. 102–113, 2009.

SALVADORI, V.O.; MASCHERONI, R.H. Prediction of freezing and thawing times of foods by Means of a Simplified Analytical Method. **Journal of Food Engineering**, v. 13, p. 67–78, 1991.

SCHWEIGER, Gerald. **Modeling Technical Systems**. [S.l.: s.n.], 2017. `http://www.ist.tugraz.at/_attach/Publish/Motes/ModellingModelica_1.pdf`. Accessed: November 24, 2020.

SIMPSON, R; CORTÉS, C. An inverse method to estimate thermophysical properties of food at freezing temperatures: apparent volumetric specific heat. **International Journal of Food Engineering**, v. 64, p. 89–96, 2003.

SUCCAR, J. C.; HAYAKAWA, K. Parametric analysis for predicting freezing time of infinitely slab-shaped food. **Journal of Food Science**, v. 49, p. 468–477, 1984.

TRUJILLO, F.J.; PHAM, Q.T. A computacional fluid dynamic model of the heat and moisture transfer during beef chilling. **International Journal of Refrigeration**, v. 29, p. 998–1009, 2006.

WHEELER, D. J.; LYDAY, R. W. **EMP Evaluating the measurement process**. [S.l.]: SPC Press, 1989.

ZILIO, C et al. Analysis of the freezing time of chicken breast finite cilinders. **International Journal of Refrigeration**, v. 95, p. 38–50, 2018.

Appendix

APPENDIX A – MSE - MEASUREMENT SYSTEM EVALUATION

A MSE (Measurement System Evaluation) was performed to verify if the measurement system was able to measure what was intended. In order for the MSE to be approved five items need to be validated: discrimination, reproducibility, repeatability, accuracy and stability. In order to be able to evaluate the MSE, control charts need to be created. The first chart built considers position as the sample label and is shown in figure 20.

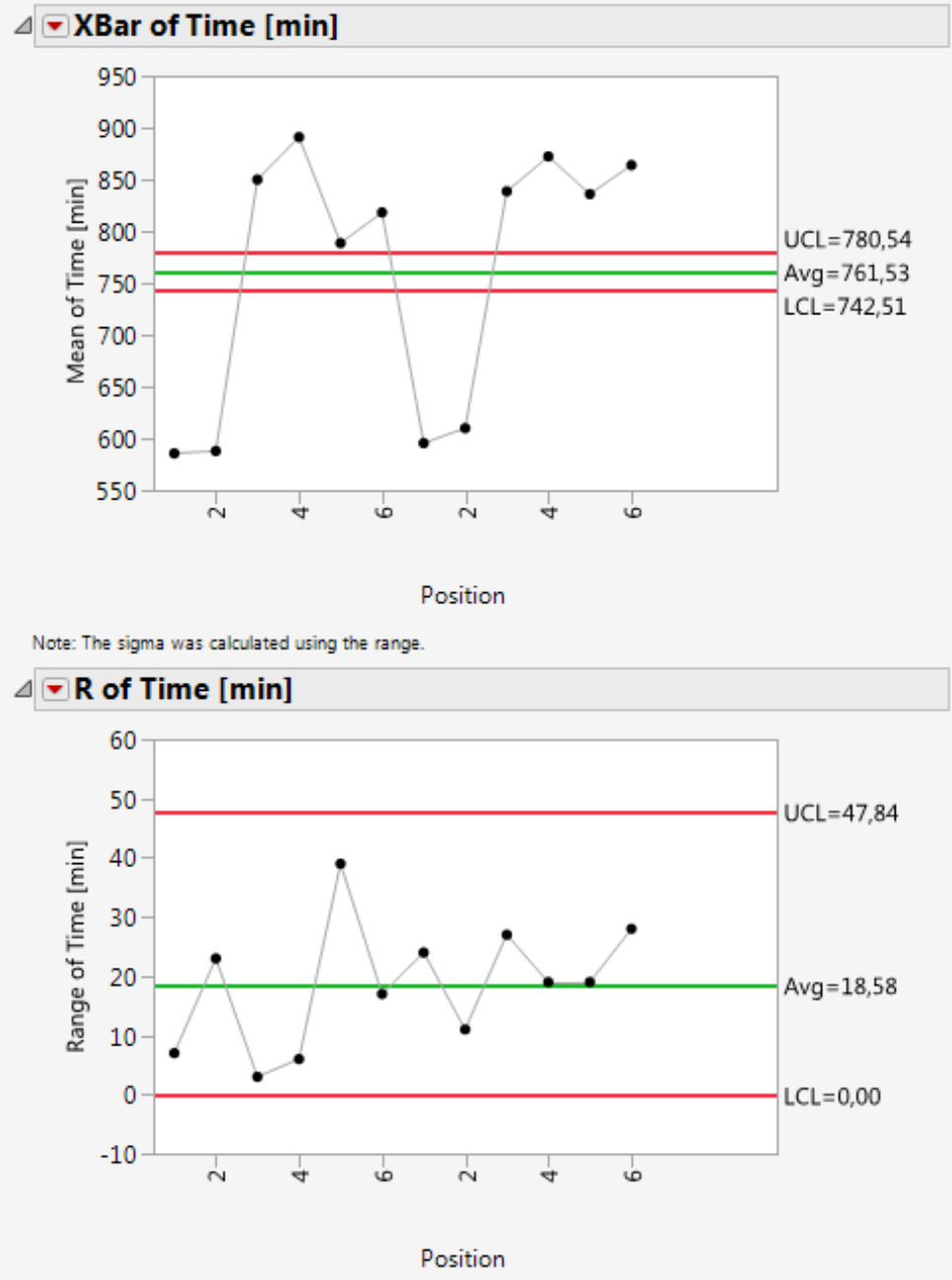

Figure 20 – Control charts ($\bar{X}$ and R) - Sample label: position

Discrimination is the system technological ability to differentiate repeated mea-

surements. This is evaluated through an equation

$$N = \frac{UCL}{\Delta} + 1 \tag{20}$$

where N is the number of measurement units, UCL is the upper control limit and Δ is the smallest difference between points observed in R (Range) chart of two non-consecutive measurements.

For the chart R in figure 20, the smallest difference is 1 for the points in the positions 3 and 6 at the right end of the chart. In this case, the number of measurement units is 48 and to evaluate if this number is enough to approve discrimination, it need to be compared to the minimum number of measurement units for the subgroup size, shown in table 16.

Table 16 – Minimum number of measurement units according to subgroup size

Subgroup Size	Minimum Number of Measurement Units
2	4
3	5
4	5
5	5
6	6

For chart in figure 20 the subgroup size is 3, because it is considering the group under the level Position in the sampling tree (image 6). So comparing to table 16, 48 > 5, approving the discrimination.

Reproducibility evaluates if there are systematic effects in the measurements. Looking at the variability chart it is observed a systematic effect of position, where positions 1 and 2 have lower averages than the others. However, in this case this effect was expected since the different positions have different airflow around the packages and therefore a different UA. Since the systematic effect was expected the reproducibility can be considered approved.

Repeatability evaluates if the measurement system is able to measure a variable with less variation than the existing variation among all the items being measured. It refers to the existing variation inside of a subgroup in a MSE. The evaluation is done through the $\bar{X}$ chart, however since the different positions measured have different averages, the chart in image 20 would not allow the correct evaluation. So, the chart in image 20 was separated by position, as shown in the figures 21 to 26.

Before any study of the $\bar{X}$ chart can be executed, an analysis of the R chart needs to be done to ensure that this chart is SPC (Stable, Predictable and Consistent). In order to be stable, all the points need to be inside the control limits of the chart and evaluating the figures 21 to 26 we can check that all points are. To be predictable the chart should allows us to predict where the next point should be if more measurements were performed, which in the charts can be expected to be inside the control limits. Consistent can be evaluated ensuring that there are no patterns being formed in the

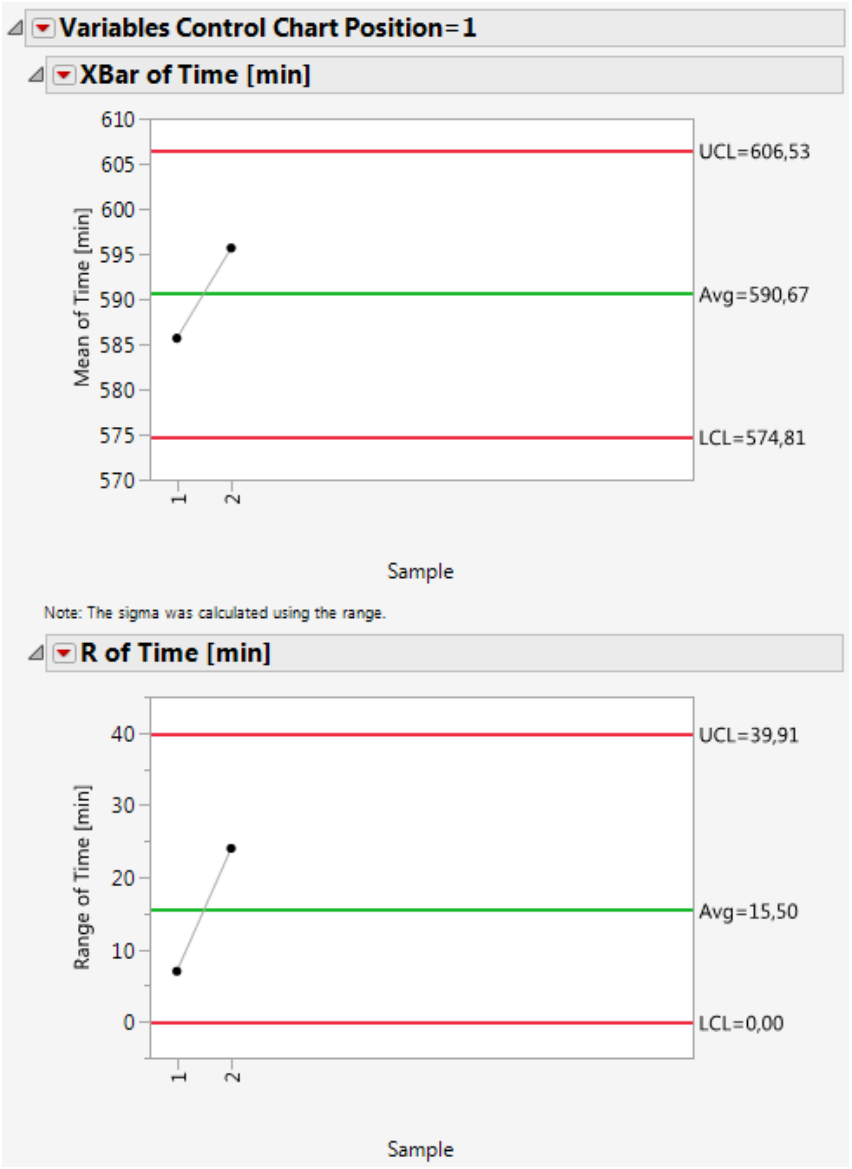

Figure 21 – Control charts ($\bar{X}$ and R) for position 1 - Sample label: Sample

measurements. Even though there are only two points in the charts, it is possible to see that the points did not form the same pattern between each position chart. Therefore all charts can be considered SPC.

Proceeding to the evaluation the $\bar{X}$ charts it shows that all the points are inside the control limits, this means that we cannot distinguish between measurements and since the packages are also the measurement instrument, then it is not possible to differentiate the packages among them. Not being able to distinguish between packages means that they are very similar in terms of freezing time.

Accuracy is the difference between the measurements average value of a variable and a standard value. Usually this item is difficult to approve since few variables have standard values available, so in order to have some information about how correct measurements are the calibration of the instruments will be considered here. Since the

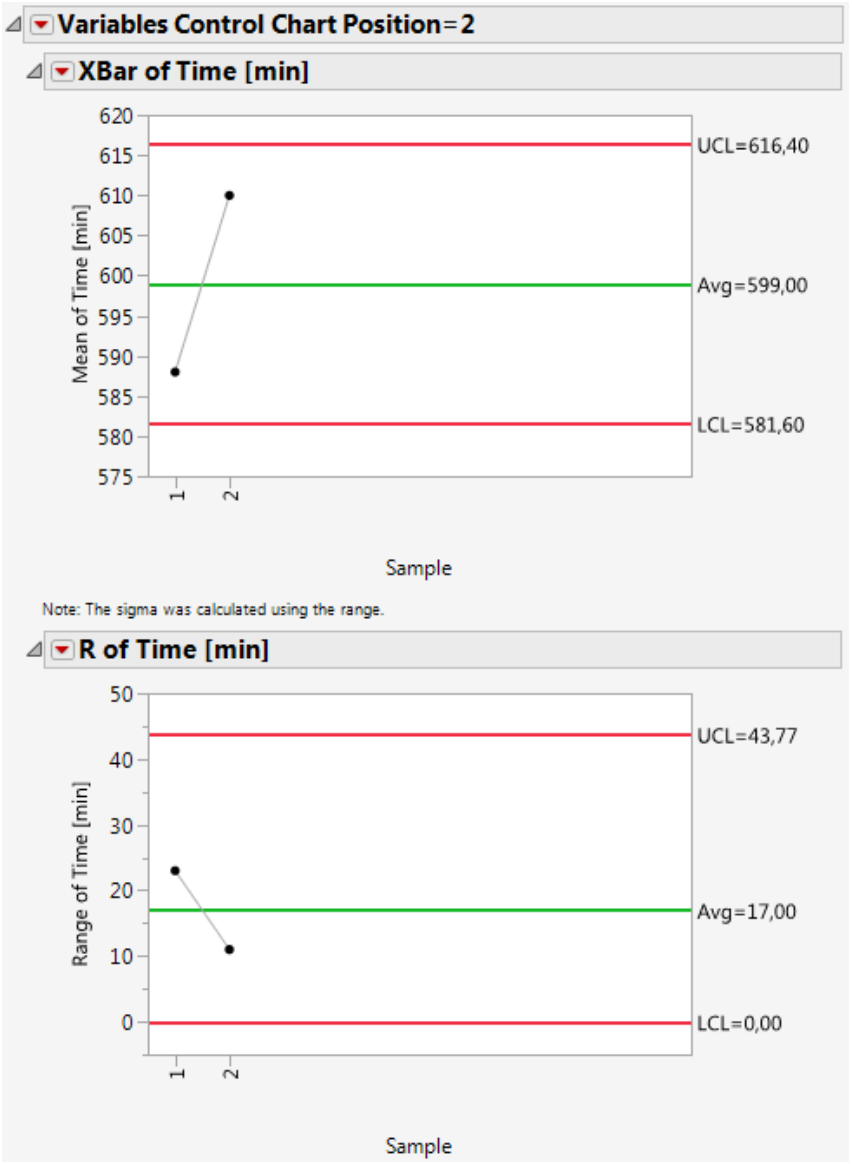

Figure 22 – Control charts ($\bar{X}$ and R) for position 2 - Sample label: Sample

thermocouples used in the tests were calibrated, accuracy will be considered approved.

Stability evaluates if the measurement system is able to measure the same items very similarly after a period of time. This item was not evaluated since a single round of tests were performed.

After evaluating the five items, it can be concluded that the MSE is approved.

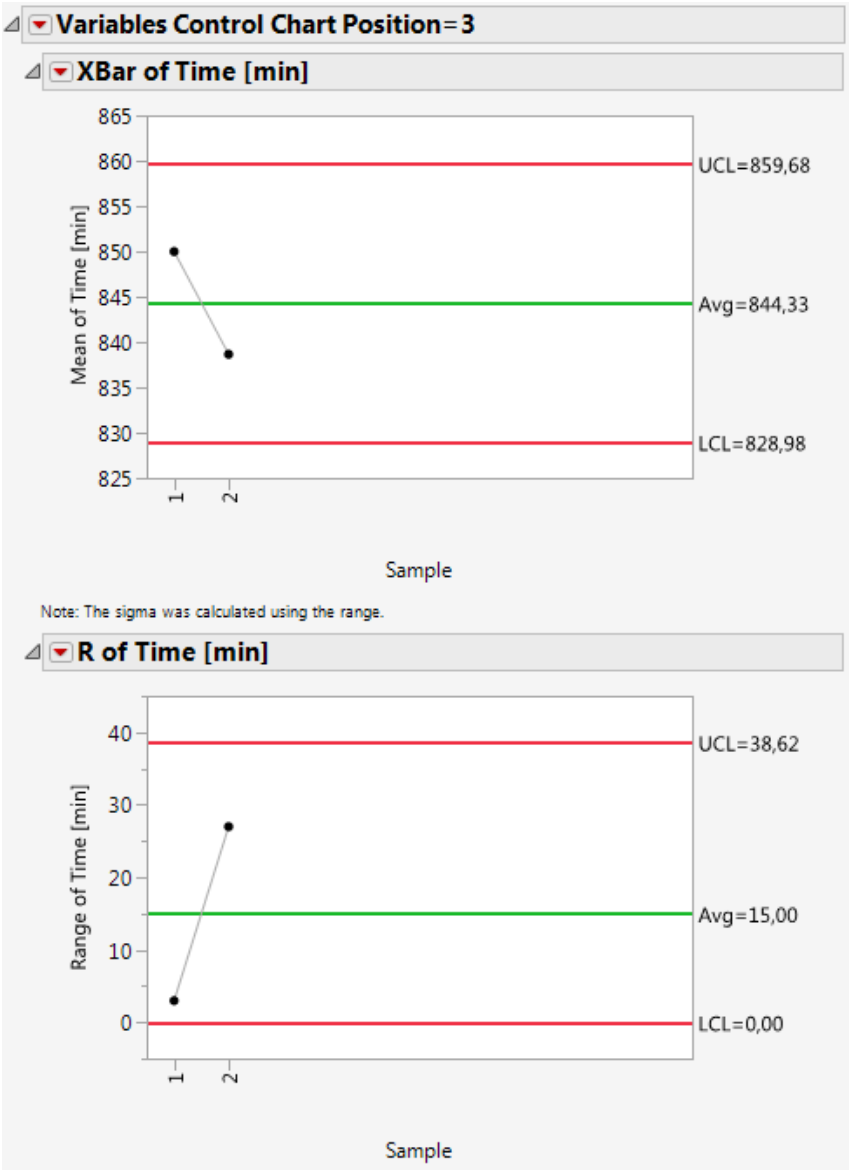

Figure 23 – Control charts ($\bar{X}$ and R) for position 3 - Sample label: Sample

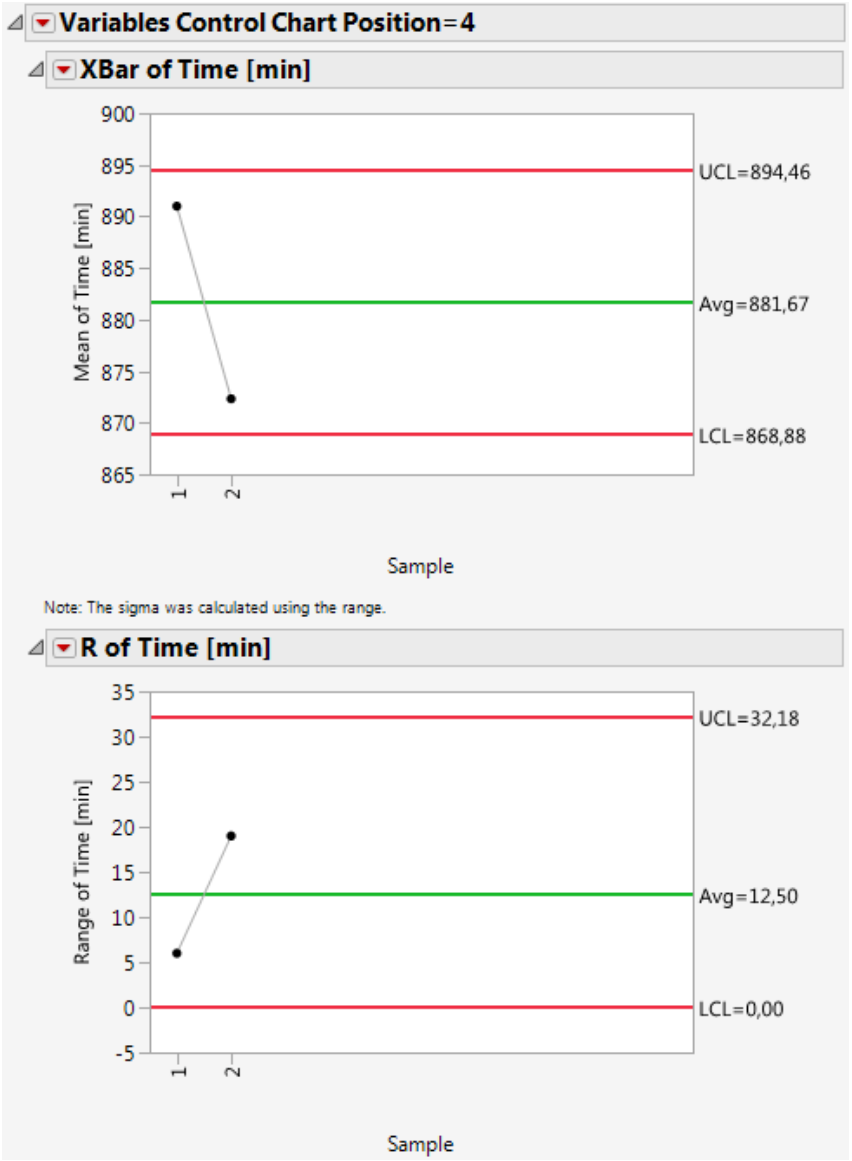

Figure 24 – Control charts ($\bar{X}$ and R) for position 4 - Sample label: Sample

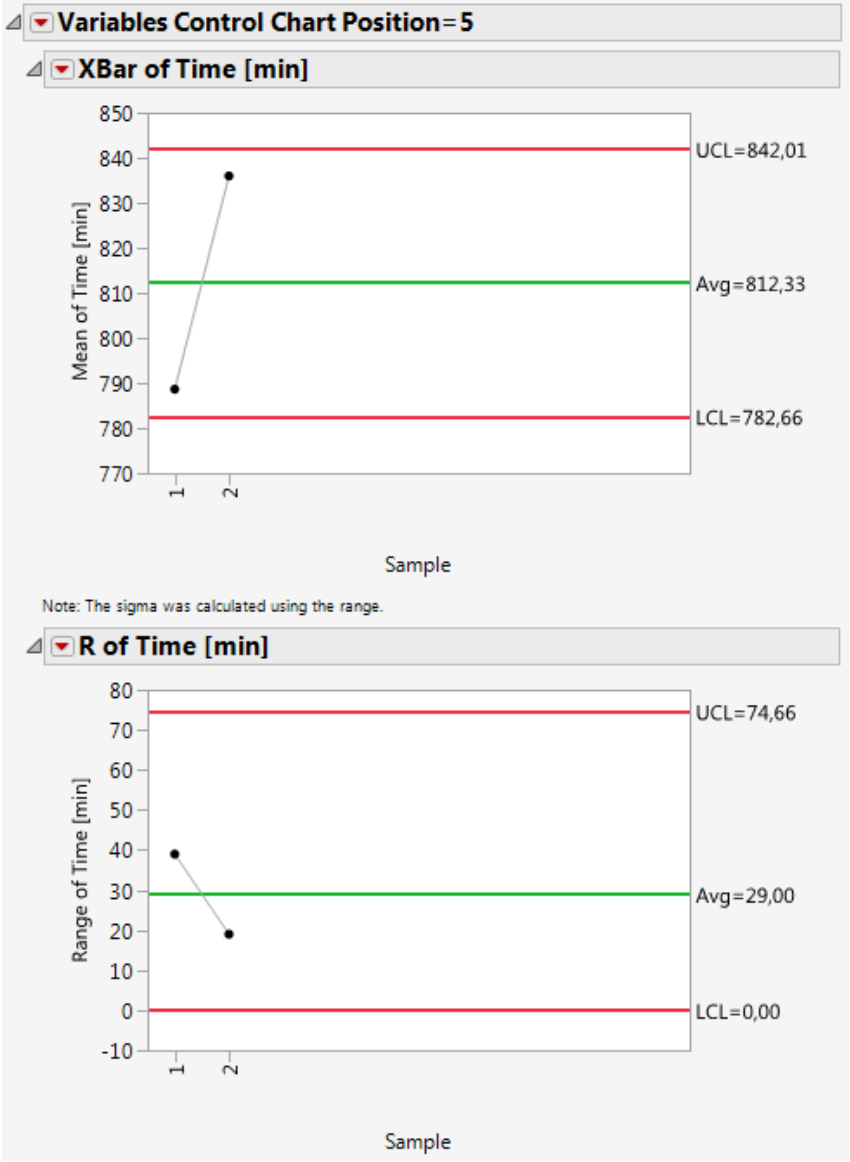

Figure 25 – Control charts ($\bar{X}$ and R) for position 5 - Sample label: Sample

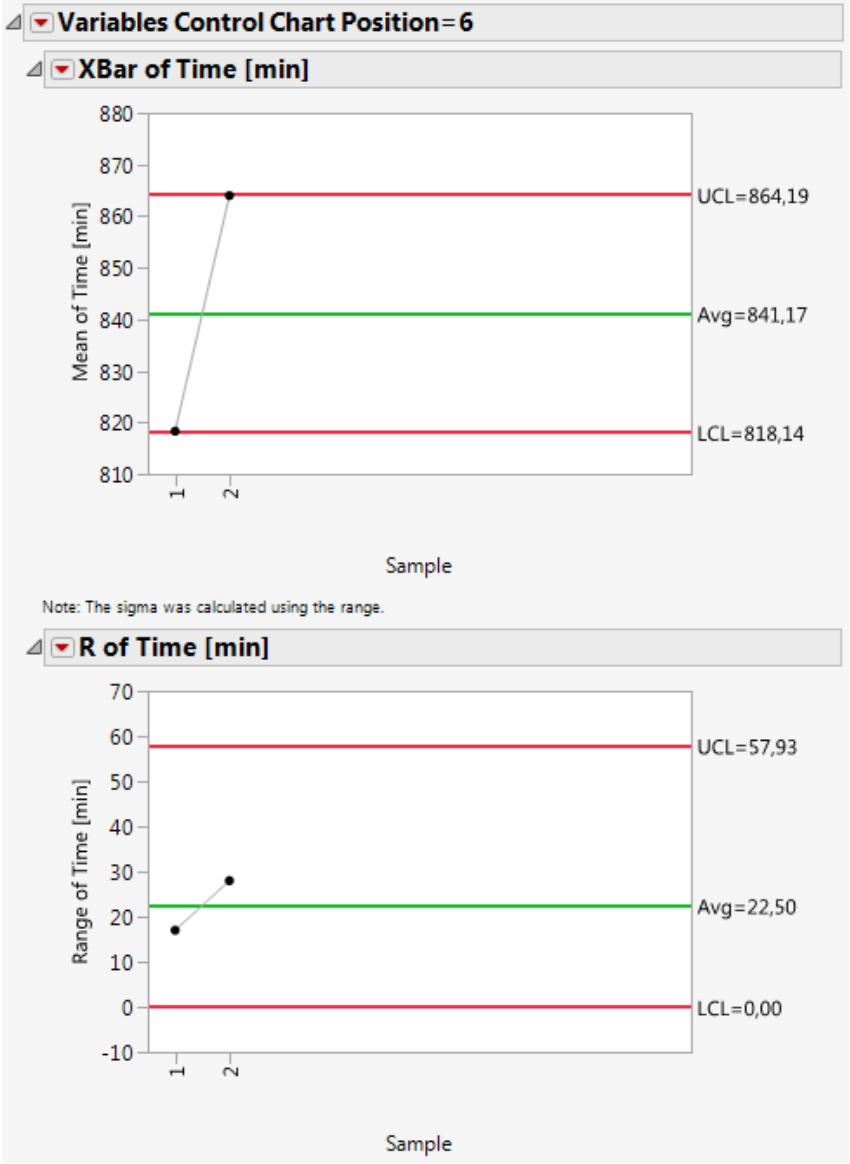

Figure 26 – Control charts ($\bar{X}$ and R) for position 6 - Sample label: Sample

APPENDIX B – THERMAL CAPACITOR CONDITIONAL EQUATIONS

```
model loadThermalCapacitor
  "Lumped thermal element storing heat and changing phase at specified temperature"
  parameter Modelica.SIunits.Mass M;
  parameter Modelica.SIunits.Temperature Tsl
    "Phase Change Temperature";
  parameter Modelica.SIunits.TemperatureDifference DTs
    "Solidification Temperature Range";
  Modelica.SIunits.SpecificHeatCapacity Cp "Specific Heat";
  parameter Modelica.SIunits.SpecificEnthalpy Hsl
    "Latent heat of Solidification";
  parameter Modelica.SIunits.SpecificHeatCapacity Cpl
    "Specific Heat of liquid";
  parameter Modelica.SIunits.SpecificHeatCapacity Cps
    "Specific Heat of solid";
  Real fs "Liquid mass fraction";
  Modelica.SIunits.Temperature T(start = 293.55, displayUnit = "degC")
    "Temperature of element";
  Modelica.SIunits.TemperatureSlope der_T(start = 0)
    "Time derivative of temperature (= der(T))";
  Modelica.Thermal.HeatTransfer.Interfaces.HeatPort_a port annotation (
    Placement(transformation(origin = {0, -100}, extent = {{-10, -10}, {10, 10}},
    rotation = 90)));

T = port.T;
der_T = der(T);

if ((T > Tsl - 0.5*DTs) and (T <= Tsl + 0.5*DTs)) then
    Cp = Hsl/DTs;
    fs = (T - (Tsl - 0.5*DTs))/DTs;
else
if (T <= Tsl - 0.5*DTs) then
      Cp =  Cps;
      fs =  0;
else
      Cp =  Cpl;
      fs = 1;
end if;
```

```
end if;

M*Cp*der(T) = port.Q_flow;

end loadThermalCapacitor;
```

APPENDIX C – THERMAL CONDUCTOR CONDITIONAL EQUATIONS

```
model loadThermalConductor
  "Lumped thermal element transporting heat without storing it"
  extends Modelica.Thermal.HeatTransfer.Interfaces.Element1D;
  parameter Modelica.SIunits.ThermalConductivity kl
    "Thermal Conductivity at Liquid State";
  parameter Modelica.SIunits.ThermalConductivity ks
    "Thermal Conductivity at Solid State";
  parameter Modelica.SIunits.Area A;
  parameter Modelica.SIunits.Length L;
  parameter Modelica.SIunits.Temperature Tsl
    "Phase Change Temperature";
  parameter Modelica.SIunits.TemperatureDifference DTs
    "Solidification Temperature Range";
  Real fs "Liquid mass fraction";
  Modelica.SIunits.ThermalConductivity k;
  Modelica.SIunits.Temperature Ta;
  Modelica.SIunits.Temperature Tb;
  Modelica.SIunits.Temperature T;

equation
  Ta = port_a.T;
  Tb = port_b.T;
  T = (Ta + Tb) / 2;
  if ((T > Tsl - 0.5*DTs) and (T <= Tsl + 0.5*DTs)) then
    fs = (T - (Tsl - 0.5*DTs))/DTs;
    k = fs*kl + (1 - fs)*ks;
  else
    if (T <= Tsl - 0.5*DTs) then
      fs =  0;
      k = fs*kl + (1 - fs)*ks;
    else
      fs = 1;
      k = fs*kl + (1 - fs)*ks;
    end if;
  end if;
  Q_flow = k * (A / L) * dT;
```

```
end loadThermalConductor;
```

APPENDIX D – CONVECTION EQUATIONS

```
model Convection
  "Lumped thermal element for heat convection (Q_flow = Gc*dT)"
  Modelica.SIunits.HeatFlowRate Q_flow "Heat flow rate from solid -> fluid";
  Modelica.SIunits.TemperatureDifference dT "= solid.T - fluid.T";
  parameter Modelica.Blocks.Interfaces.RealInput UA(unit = "W/K")
    "Signal representing the convective thermal conductance in [W/K]"
    Placement(transformation(origin = {0, 100}, extent = {{-20, -20}, {20, 20}},
    rotation = 270)));
  Modelica.Thermal.HeatTransfer.Interfaces.HeatPort_a solid annotation (
    Placement(transformation(extent = {{-110, -10}, {-90, 10}})));
  Modelica.Thermal.HeatTransfer.Interfaces.HeatPort_b fluid annotation (
    Placement(transformation(extent = {{90, -10}, {110, 10}})));
equation
  dT = solid.T - fluid.T;
  solid.Q_flow = Q_flow;
  fluid.Q_flow = -Q_flow;
  Q_flow = UA * dT;

end Convection;
```

APPENDIX E – STANDARD DEVIATION ANALYSIS FOR THE TIME INTERVALS

For the time intervals presented in the table 10 the sample tree is shown in figure 27. This shows a simplified tree due to the quantity of time intervals that if displayed completely would be too large.

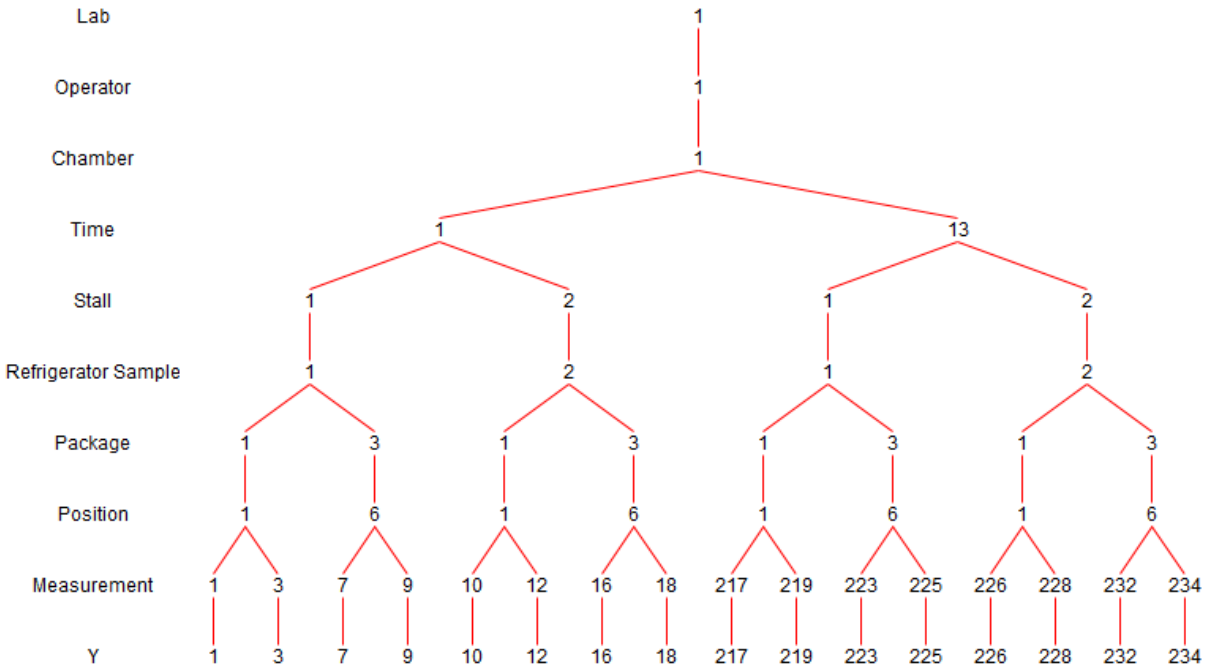

Figure 27 – Sample tree for temperature evaluation along the time

The mean and ranges for the subgroup measurement was calculated and it is shown in the charts in figures 28 and 29 respectively. In the top chart from figure 29 it can be seen that the ranges are different depending on the temperature being evaluated, looking at top chart in figure 28 it shows that there is a smaller variation in for the points in the phase change portion.

So the data for this portion was evaluated separately and its shown in image 30, the standard variation calculated for the temperatures measured between 0°C and -2.5°C is 0.2°C and experimental measurement uncertainty is 0.4°C.

Taking the data for the temperatures higher than 0°C and lower than -2.5°C the means and ranges were calculated and are shown in image 31. Looking at the chart for the range it looks like it the positive and negatives temperatures may have different ranges, one being higher than other so the data was separated between positive and negative portions and new charters were created for the means and ranges displayed in images 32 and 33 for positive and negative subsets respectively.

For the positive temperatures the calculated standard deviation is 0.3°C and the experimental measurement uncertainty is 0.6°C. For the negative subset the calculated standard deviation is 0.5°C and the experimental measurement uncertainty is 1.0°C.

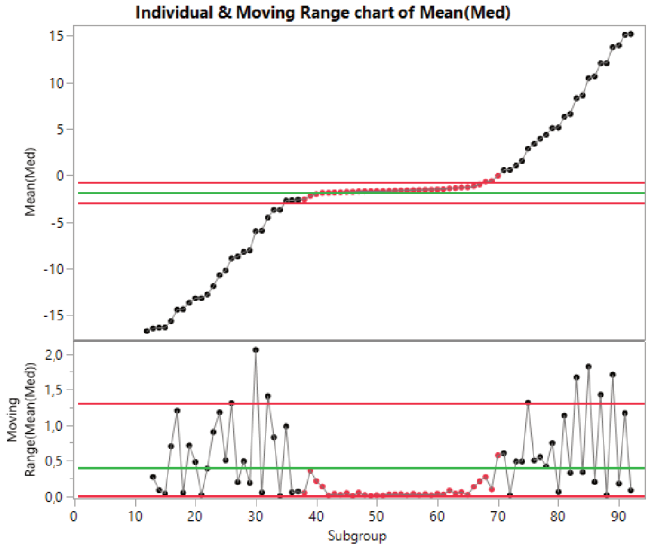

Mean(Med) Limit Summaries

Points plotted	LCL	Avg	UCL	Limits Sigma	Subgroup Size
Individual	-2,92207	-1,86148	-0,80089	Moving Range	.
Moving Range	0	0,398917	1,303074	Moving Range	.

Figure 28 – Individual Moving Range (IM and R) control charts for the mean of the subgroup measurement

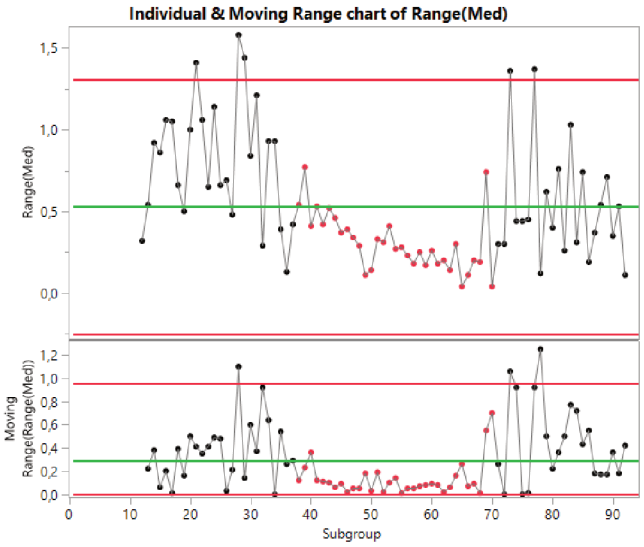

Range(Med) Limit Summaries

Points plotted	LCL	Avg	UCL	Limits Sigma	Subgroup Size
Individual	-0,24804	0,530617	1,309278	Moving Range	.
Moving Range	0	0,292875	0,956686	Moving Range	.

Figure 29 – Individual Moving Range (IM and R) control charts for the range for the subgroup measurement

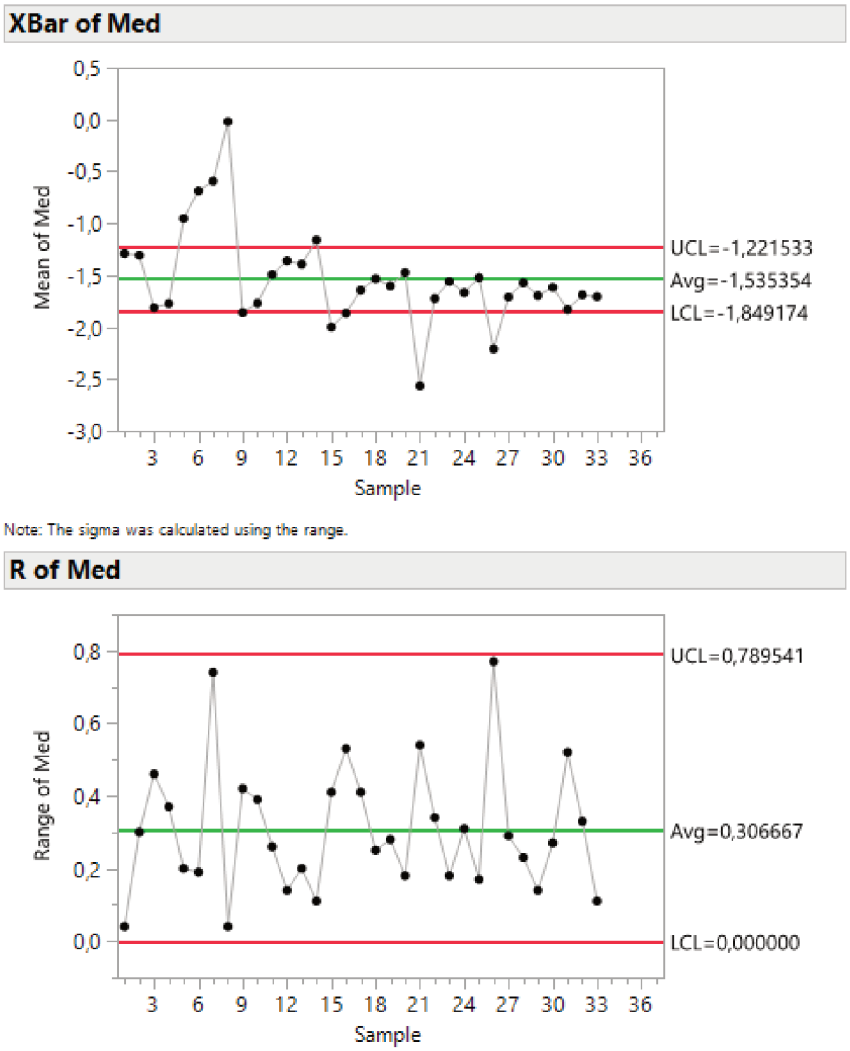

Figure 30 – Control charts ($\bar{X}$ and R) for the temperatures between 0°C and -2.5°C for the subgroup measurement

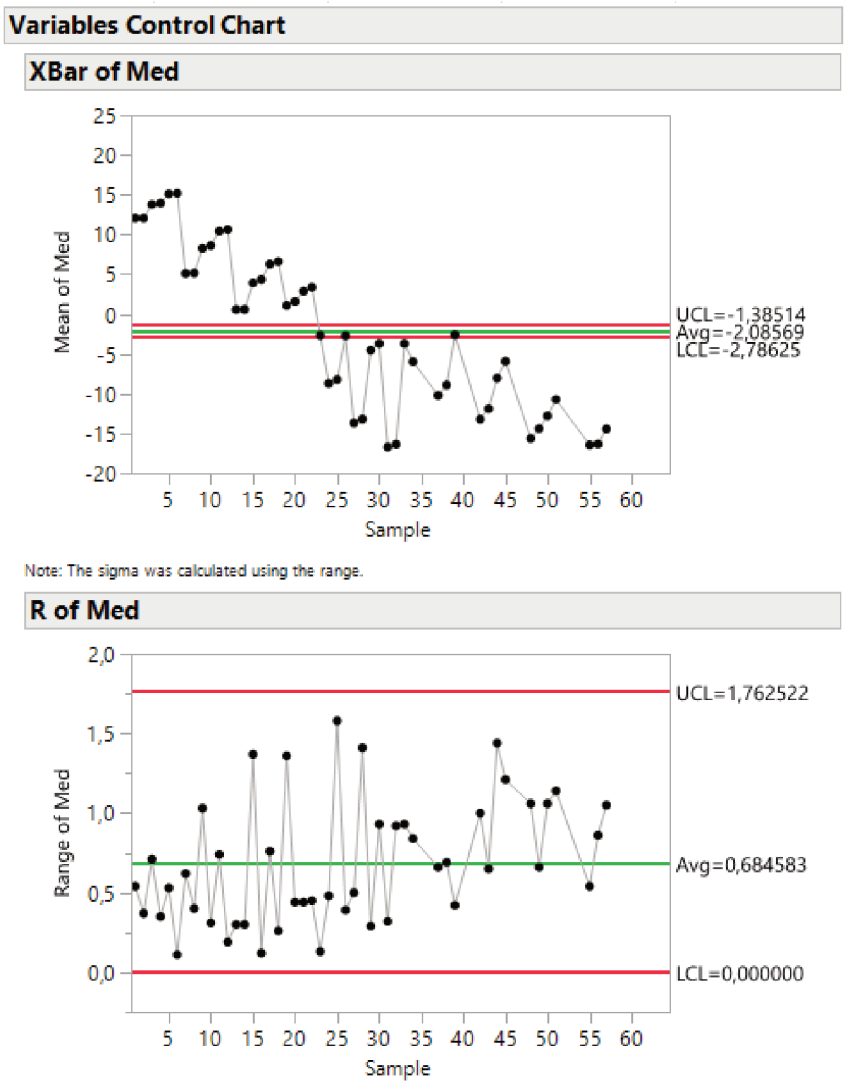

Figure 31 – Control charts ($\bar{X}$ and R) for the temperatures higher than 0°C and lower than -2.5°C for the subgroup measurement

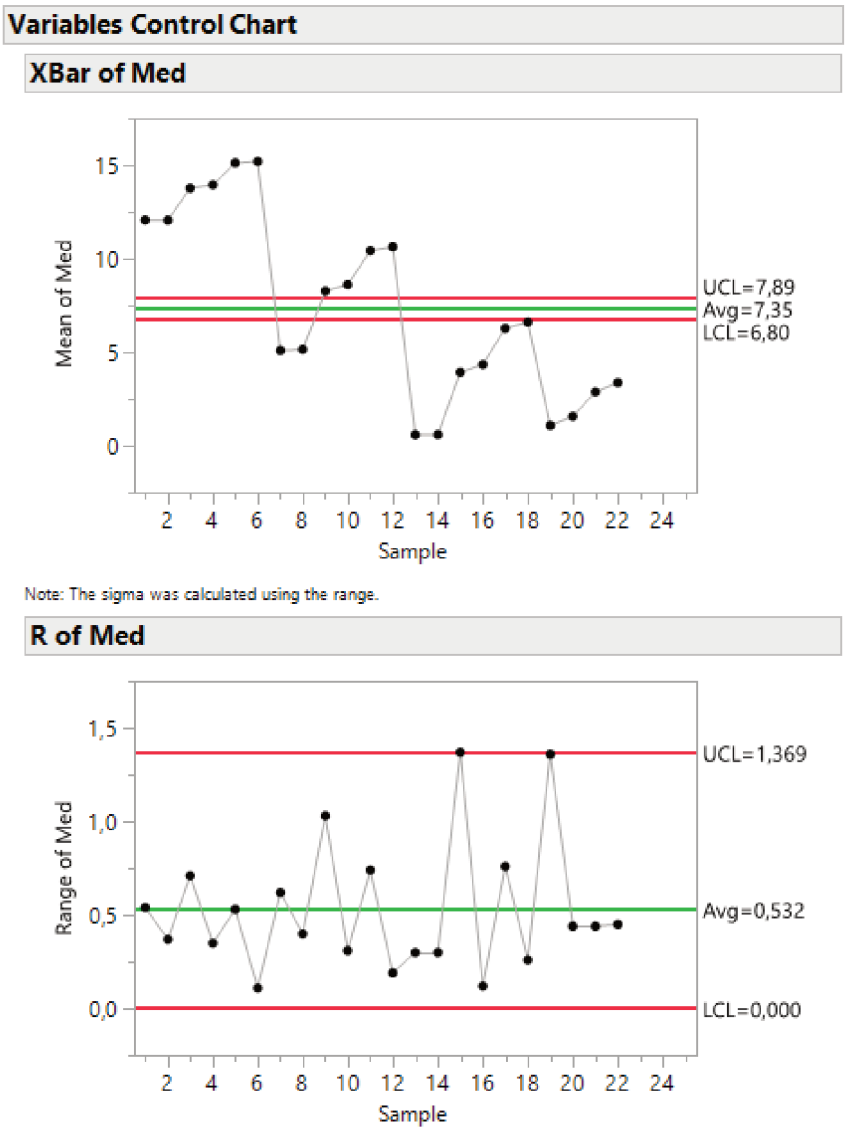

Figure 32 – Control charts ($\bar{X}$ and R) for the temperatures higher than 0°C for the subgroup measurement

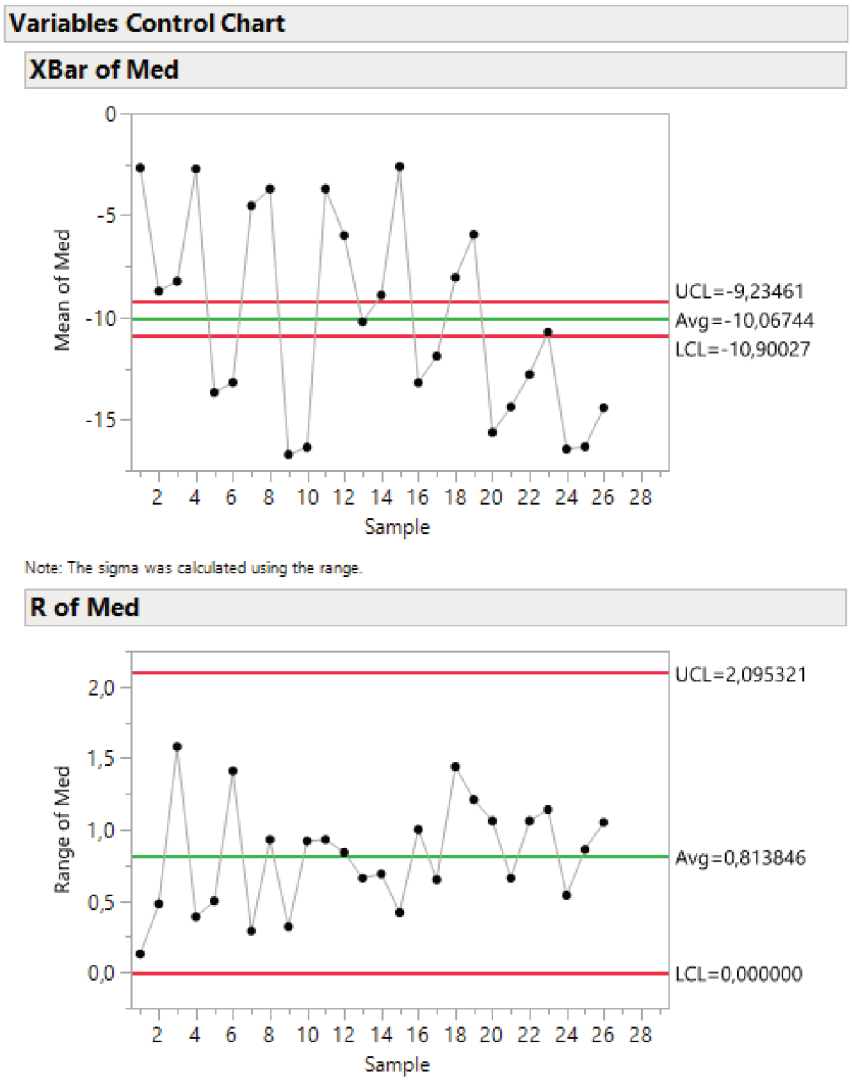

Figure 33 – Control charts ($\bar{X}$ and R) for the temperatures lower than -2.5°C for the subgroup measurement

APPENDIX F – HEAT TRANSFER VALUES FOR MESH REFINEMENT TESTS

Table 17 – Position 01 Heat Transfer Values (W)

Position 01	Top	Right	Left	Front	Bottom	Back
Test 01	0.31324	0.20121	0.17264	0.24259	0.36066	0.24283
Test 02	0.32911	0.20495	0.17397	0.25545	0.35580	0.22793
Test 03	0.35912	0.20431	0.17349	0.25041	0.35804	0.24023
Test 04	0.34111	.20153	0.16901	0.24791	0.35152	0.24094

Table 18 – Position 02 Heat Transfer Values (W)

Position 02	Top	Right	Left	Front	Bottom	Back
Test 01	0.38401	0.14806	0.29657	0.20308	0.32167	0.17386
Test 02	0.39180	0.14914	0.29510	0.20296	0.32582	0.17408
Test 03	0.39323	0.15209	0.30121	0.20878	0.32841	0.17211
Test 04	0.38599	0.15617	0.30042	0.20629	0.32235	0.17362

Table 19 – Position 03 Heat Transfer Values (W)

Position 03	Top	Right	Left	Front	Bottom	Back
Test 01	0.46882	0.21911	0.18139	0.30974	-	0.12681
Test 02	0.47701	0.22003	0.17776	0.31022	-	0.12825
Test 03	0.48591	0.22545	0.17776	0.30916	-	0.12736
Test 04	0.47776	0.22022	0.17704	0.30896	-	0.12580

Table 20 – Position 04 Heat Transfer Values (W)

Position 04	Top	Right	Left	Front	Bottom	Back
Test 01	-	0.17032	0.12119	0.26990	0.11809	0.09358
Test 02	-	0.16580	0.12548	0.26498	0.11603	0.09417
Test 03	-	0.17134	0.12668	0.26950	0.11308	0.09439
Test 04	-	0.17147	0.12343	0.26670	0.11470	0.09689

Table 21 – Position 05 Heat Transfer Values (W)

Position 05	Top	Right	Left	Front	Bottom	Back
Test 01	0.36214	0.11573	0.21866	0.19425	-	0.13728
Test 02	0.35867	0.11613	0.22221	0.20614	-	0.14139
Test 03	0.36902	0.11748	0.22706	0.21372	-	0.14112
Test 04	0.36398	0.11701	0.22390	0.20487	-	0.14082

Table 22 – Position 06 Heat Transfer Values (W)

Position 06	Top	Right	Left	Front	Bottom	Back
Test 01	-	0.11140	0.22659	0.21620	0.08825	0.11820
Test 02	-	0.11227	0.22977	0.21946	0.08614	0.11584
Test 03	-	0.11351	0.23083	0.21927	0.08468	0.11942
Test 04	-	0.11184	0.23215	0.21406	0.08555	0.11664

APPENDIX G – STANDARD DEVIATION ANALYSIS FOR THE FREEZER TEMPERATURE

The sample tree for the freezer air temperature measurements is presented in figure 34.

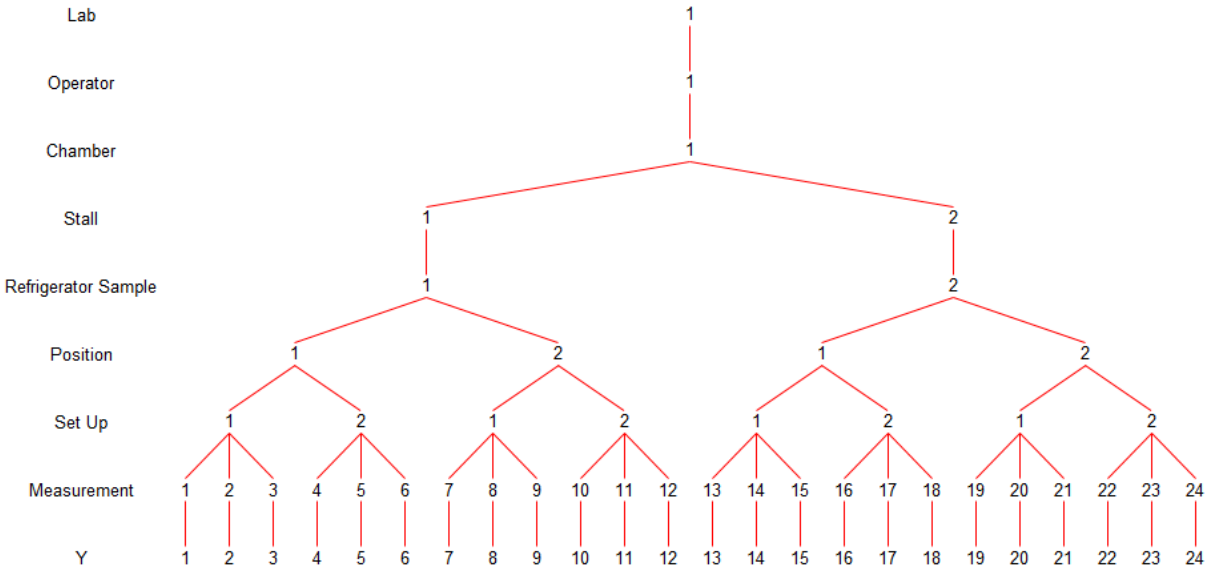

Figure 34 – Sampling tree for freezer air temperature

An analysis of the mean and range of the freezer air temperature measurements is shown in figure 35. With this data the standard deviation calculated is 0.2°C and the total experimental measurement uncertainty is 0.4°C.

—

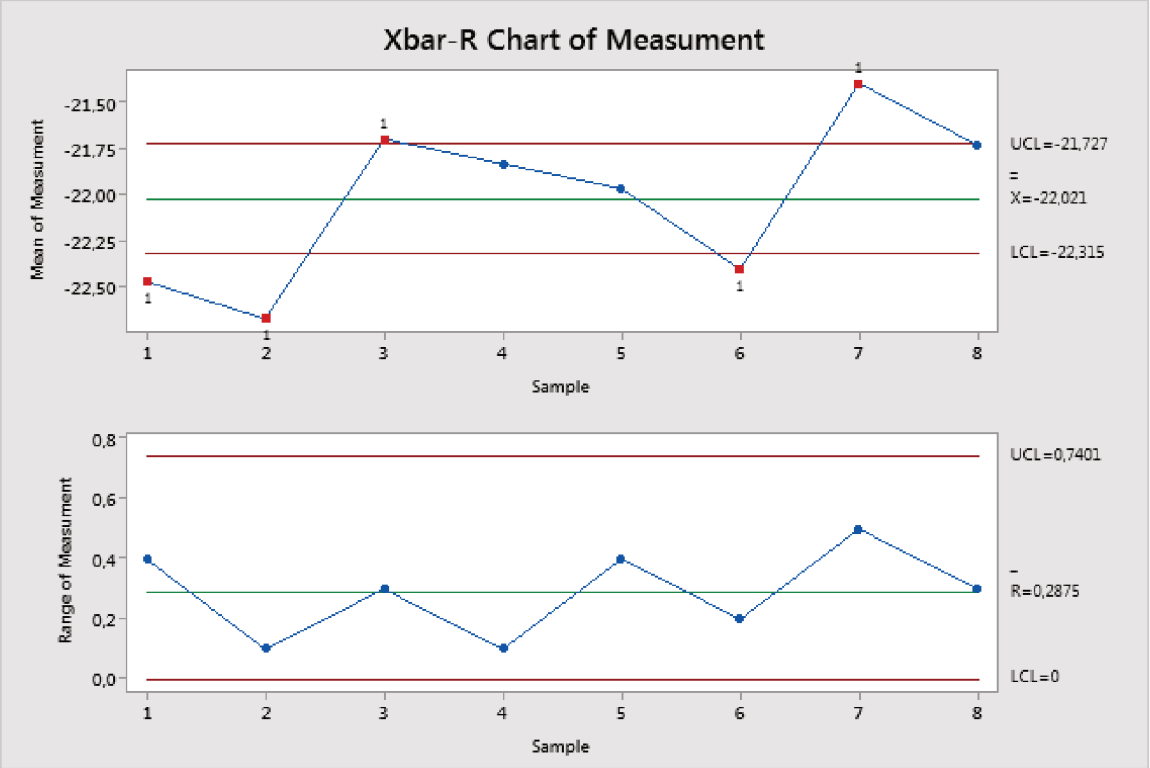

Figure 35 – Control charts ($\bar{X}$ and R) for the freezer air temperature for the subgroup measurement